Geologic map of the southern part of the Vail 7.5' Quadrangle, eastern Pima County, Arizona

by

Stephen M. Richard, Jon E. Spencer, Charles A. Ferguson, and Ann Youberg

Arizona Geological Survey Digital Geologic Map 12

July, 2002 (Revised)

Scale 1:24,000 (1 sheet), with 29 page text

Arizona Geological Survey
416 W. Congress St., #100, Tucson, Arizona 85701

Research partially supported by the U.S. Geological Survey, National Cooperative Geologic Mapping Program, under USGS award number #00HQAG0149. The views and conclusions contained in this document are those of the authors and should not be interpreted as necessarily representing the official policies, either expressed or implied, of the U.S. Government.

Revisions.
December, 2001. Original release
July, 2002. Update stratigraphic terminology for Pantano and Bisbee Formations, change map colors to match adjacent quadrangles, generate new pdf files.

TABLE OF CONTENTS

Table of Contents i
Introduction 1
Quaternary Geology 2
Methodology 3
Geologic/Geomorphic Framework 4
Geologic Hazards 5
Structural Geology 8
Mineral deposits 9
Silicification 10
Rock Units 11
Quaternary and Late Tertiary map units 11
Piedmont Alluvium 11
Axial Stream Deposits 15
Hillslope Deposits 16
Tertiary map units 16
Pantano Formation (Oligocene to Miocene) 17
Tertiary igneous rocks 20
Mesozoic map units 20
Bisbee Group 20
Paleozoic map units 21
Proterozic map units 24
Apache Group and associated Sierra Ancha diabase 24
Early to Middle Proterozoic crystalline rock units 24
References Cited 25

INTRODUCTION

The study area is located ~40 km southeast of downtown Tucson, and is bounded by the Rincon Mountains on the north, the Empire Mountains on the southeast, and the northernmost Santa Rita Mountains on the southeast. The map area covers the southern part of the Vail 7 ½' Quadrangle, including all the Paleozoic rocks in the Colossal Cave area. Field mapping was completed during October 2000 through April 2001 as part of a multiyear mapping program directed at producing complete geologic map coverage for the Phoenix-Tucson metropolitan corridor. A 1:24,000 scale map is the primary product of this study (Plate 1). This map consists almost entirely of new mapping but locally incorporates data from published mapping by other workers. The accompanying report describes rock units and other geologic features. This mapping was done under the joint State-Federal STATEMAP program, as specified in the National Geologic Mapping Act of 1992. Mapping was jointly funded by the Arizona Geological Survey and the U.S. Geological Survey under STATEMAP Program Contract #00HQAG0149.

The bedrock geology of the map area is dominated by several groups of rock units, as follows: (1) Complexly deformed Paleozoic carbonate and siliciclastic strata, Proterozoic siliciclastic sediments of the Apache Group, and underlying granitoids and diabase in the northeastern part of the map area. These rocks form the southwestern edge of the Rincon Mountains, and lie above the late Oligocene to early Miocene Catalina detachment fault, a moderately to gently southwest dipping normal fault that has tens of kilometers of displacement (>27.5 km displacement estimated by Dickinson, 1991). (2) The Oligo-Miocene Pantano Formation, which consists of variably tilted conglomerate, sandstone, mudstone, and andesitic lava flows. (3) Sandy siliciclastic sedimentary rocks of the lower Bisbee Group that depositionally overly Proterozoic granitoid in the southeastern corner of the map area.

Quaternary stream incision has uncovered unconsolidated to poorly consolidated clastic sedimentary deposits of uncertain age and affinity that are typically mantled by colluvium. In many areas these deposits are shown on plate 1 as Tertiary and Quaternary deposits, undivided.

Table 1: Vail area, theses and dissertations

Acker, C.J., 1958, Geologic interpretations of a siliceous breccia in the Colossal Cave area, Pima County, Arizona: Tucson, University of Arizona, M.S. thesis, 50 p.

Alberding, H., 1938, Geology of the northern Empire Mountains, Arizona: Tucson, University of Arizona, Ph.D. dissertation, 107 p.

Balcer, R.A., 1984, Statigraphy and depositional history of the Pantano Formation (Oligocene-early Miocene), Pima County, Arizona: Tucson, University of Arizona, M.S. thesis, 107 p.

Bittson, A.G., 1976, Analysis of gravity data from the Cienega Creek area, Pima and Santa Cruz Counties, Arizona: Tucson, University of Arizona, M.S. thesis, 76 p., 5 sheets, scale 1:62,500.

Brennan, D.J., 1957, Geological reconnaissance of Cienega Gap, Pima County, Arizona: Tucson, University of Arizona, Ph.D. dissertation, 53 p.

Grimm, J.P., 1978, Cenozoic pisolitic limestones of Pima and Cochise Counties, Arizona: Tucson, University of Arizona, M.S. thesis, 71 p.

Janders, D.J., 1978, Comparative sedimentology, stratigraphy and economic potential of two Tertiary lacustrine deposits in Arizona: Tempe, Arizona State University, M.S. thesis.

Layton, D.W., 1957, Stratigraphy and structure of the southwestern foothills of the Rincon Mountains, Pima County, Arizona: Tucson, University of Arizona, M.S. thesis, 87 p.

Metz, R.A., 1963, The petrography of the Pantano Beds in the Cienega Gap area, Pima County, Arizona: Tucson, University of Arizona, M.S. thesis, 66 p.

Weidner, M.I., 1957, Geology of the Beacon Hill-Colossal Cave area, Pima County, Arizona: Tuc-

Mineralization in the map area is restricted to several small prospects along faults zones cutting Paleozoic rocks.

Previous mapping. The Vail 7 ½' Quadrangle was mapped previously as part of a 1:48,000 scale map of the map of the Rincon Valley 15' Quadrangle [Drewes, 1977]. Several topical studies, some including mapping, have been done as part of M.S. and Ph.D. thesis projects (Table 1).

Acknowledgments. We especially thank Bill Peachy for providing access to the Colossal Cave area.

QUATERNARY GEOLOGY

This report and accompanying map describes the surficial geology, geomorphology, and geologic hazards of the Vail 7.5' quadrangle located on the eastern fringe of the Tucson metropolitan area. The mapping area is in unincorporated Pima County, but it includes the rapidly growing Vail area. Potentially conflicting land use issues in the area include rapid urban development and population growth, national forest service lands, state parks lands, and traditional ranching areas. This report is intended to enhance our understanding of the surficial geology of the area and to aid in assessing and understanding geologic hazards.

This surficial geologic mapping of the Vail quadrangle is part of a larger effort to map the surficial and bedrock geology and geologic hazards of six contiguous 7.5' quadrangles: Mount Fagan, Mount Fagan, Rincon Peak, The Narrows, Galleta Flat West and Mescal. It continues the efforts by the AZGS to map the geology of the Phoenix – Tucson urban corridor. This mapping builds on and complements previous surficial geologic mapping efforts in the Tucson area [McKittrick, 1988; Jackson, 1989; Jackson, 1990; Demsey and others, 1993; Klawon and others, 1999; Pearthree and Biggs, 1999, Pearthree and Youberg, 2001]. The report is organized into a brief introduction and explanation of mapping methods, unit descriptions, a summary of the geologic and geomorphic framework of the area, and a discussion of geologic hazards. Ann Youberg mapped and described the Quaternary geology, with assistance and suggestions from Philip A. Pearthree. Tim Orr and Steve Richard assisted with map digitization and preparing the map layouts and provided quality control for the map compilation. Ray Harris contributed to the section on ground water withdrawal and subsidence. Mapping was conducted as part of the STATEMAP Program of the U.S. Geological Survey, contract #00HQAG0149, and was supported by the Arizona Geological Survey and the U.S. Geological Survey National Cooperative Mapping Program.

Climate. Several weather stations located near the map area that have operated during intervals over the past century provide climatological data for the study area. The current Tucson Weather Service Office at Tucson International Airport (WSO, about 10 miles west of the map area) has records from 1948 to the present and the weather station maintained at the Santa Rita Experimental Range Headquarters (ERH, about 15 miles southwest of the map area) has records from 1950 to present. Stations were maintained at Benson (about 20 miles east of the map area) from 1894 to 1975, and at Helvetia (about 12 miles southwest of the map area) from 1916 to 1950. Throughout this region, most of the annual precipitation (50-60%) falls during the summer monsoon from June to September. Late summer rainfall occurs as heavy thunderstorms when moist air sweeps northwards from the Gulf of California and the Gulf of Mexico. Moist air derived from dissipating tropical storms in the Pacific Ocean produces occasional intense late summer to early fall precipitation. Cyclonic storms originating in the Pacific cause most winter precipitation. It is usually less intense and may be more prolonged, and therefore infiltrates into the soil more deeply than summer rainfall (summarized from Sellers and Hill, 1974). Freezing temperatures are common during most winters, but snow is uncommon and not persistent.

Climate records from these stations illustrate the precipitation and temperature gradients across the map area. Records from the WSO, at about 2500 ft asl, and Benson, at about 3500, show similar average annual precipitation and temperatures for slightly different time periods. Average annual precipitation is 11.6 in. for the WSO, and 11.3 in. for Benson [Western Regional Climate Center, 2001]. The average maximum temperature for the WSO is 82.5° F, with an average high temperature of 99.1° F in July and 64.7° F in January. Benson is slightly cooler. ERH and Helvetia, both near 4300 ft asl, are wetter and cooler. Average annual precipitation for the ERH and Helvetia are 22.3 and 19.7 inches, respectively, which is double the average annual precipitation for the WSO or Benson. The average maximum temperature at the ERH is 76.4° F, with average high temperatures of 91.6° F in July and 60.2° F in January. The average maximum temperature at Helvetia is 75.6° F, with average high temperatures of 91.3° F in July and 57.9° F in January. The average annual precipitation for ERH is probably a maximum for the map area because of its proximity to the base of the Santa Rita Mountains.

Methodology

The surficial geology of the project area was mapped using color 1:48000 aerial photographs taken in 1979, provided by James Briscoe of JABA LLC. Original mapping of the Vail quadrangle was conducted by Jackson [1989] and modified by Youberg for this map. Unit boundaries were spot-checked in the field, and mapping was supplemented by observations and descriptions of soils and stratigraphy. The physical characteristics of Quaternary alluvial surfaces (channels, alluvial fans, floodplains, stream terraces) evident on aerial photographs and in the field were used to differentiate their associated deposits by age. Surficial deposits of this quadrangle were then correlated with similar deposits in this region in order to estimate their approximate ages. Original mapping was done on aerial photographs, which were then registered and rectified using ERDAS Imagine. Unit boundaries were vectorized from the Imagine files using R2V and imported into Arc/Info, where the map was compiled and generated.

The physical characteristics of Quaternary alluvial surfaces (channels, alluvial fans, floodplains, stream terraces) were used to differentiate their associated deposits by age. Alluvial surfaces of similar age have a distinctive appearance and soil characteristics because they have undergone similar post-depositional modifications. They are different from both younger and older surfaces. Terraces and alluvial fans that are less than a few thousand years old still retain clear evidence of the original depositional topography, such as bars of gravel deposits, swales (trough like depressions) where low flows passed between bars, and distributary channel networks, which are characteristic of active alluvial fans. Young alluvial surfaces have little rock varnish on surface clasts and have little soil development, and they are minimally dissected. Very old fan surfaces, in contrast, have been isolated from substantial fluvial deposition or reworking for hundreds of thousands of years. These surfaces are characterized by strongly developed soils with clay-rich argillic horizons and cemented calcium-carbonate horizons, well-developed tributary stream networks that are entrenched 1 to 10 m below the fan surface, and strongly developed varnish on surface rocks. The ages of alluvial surfaces in the southwestern United States may be roughly estimated based on these surface characteristics, especially soil development [Gile and others, 1981; Bull, 1991].

In this map, Quaternary surficial deposits are subdivided based on their source (axial valley streams and smaller tributary washes on piedmonts) and estimated age of deposits. Surface and soil characteristics were used to correlate alluvial deposits and to estimate their ages. Surface pits and exposures along cut banks were used to assess soil characteristics associated with deposits of different ages and from different sources. Soils and surfaces documented in the map area were generally correlated with soils and surfaces described in Quaternary mapping studies of adjacent areas conducted by Katzer and Schuster

[1984], McKittrick [1988], Jackson [1989], Jackson [1990], Demsey and others [1993], Klawon and others [1999], Pearthree and Biggs [1999], and Pearthree and Youberg [2000]. These correlations were also used to estimate the ages of surficial deposits in the map area.

Geologic/Geomorphic Framework

The Vail quadrangle is located east of the Tucson Metropolitan area along the eastern edge of the Sonoran Desert subprovince of the Basin and Range physiographic province. The Basin and Range province in Arizona is characterized by alluvial basins and intervening mountain ranges that formed as a result of normal faulting related to extension of the crust between about 30 and 6 Ma [Shafiqullah and others, 1980; Menges and Pearthree, 1989]. The landscape of the Tucson area consists of alluvial basins between large, high mountain ranges to the east and small, low-lying mountain ranges to the west. The western part of the metropolitan area (Avra Valley and the west side of the Tucson Mountains) is typical of the undissected basins that are common throughout the Sonoran Desert subprovince. Mountain ranges are low and mountain fronts are deeply embayed, with few outlying bedrock knobs (inselbergs) that rise above the broad plains surrounding the mountain ranges. Upper piedmont areas typically are covered with Pleistocene deposits that are moderately dissected, but lower piedmont areas are undissected and covered by relatively fine-grained young deposits that grade downslope into axial valley deposits. The axial portions of valleys are typically occupied by unentrenched drainages with very broad floodplains. In stark contrast, the eastern, northern, and southern parts of the Tucson area have large, high mountain ranges and piedmont areas have been deeply dissected by erosion. In these areas, erosion has dominated landscape evolution at least through the Quaternary. Major periods of aggradation have punctuated the long-term trend toward downcutting along the major streams and their tributaries, resulting in the formation of terraces along these watercourses.

The highest levels of alluvial deposits (unit QTs and QTg ridgelines) may have been graded approximately to the Tucson basin before it was significantly entrenched. They are probably approximately correlative with QT deposits mapped in the Catalina foothills on the north side of the Tucson basin [Klawon and others, 1999], Qo and QT deposits mapped in the Tucson Mountain foothills on the west side of the Tucson basin [Pearthree and Biggs, 1999], and other high remnant deposits throughout southeastern Arizona [Menges and McFadden, 1981]. It is likely that in the late Pliocene to early Quaternary, these alluvial surfaces were fairly planar, undissected piedmonts that graded downslope to a large alluvial fan complex that emanates from the Cienega Gap area westward across the Tucson basin.

Erosion has dominated landscape evolution at least through the Quaternary. Major periods of aggradation have punctuated the long-term trend toward downcutting along the major streams and their tributaries. During the past one to two million years, Pantano Wash and its tributaries have downcut substantially into the Quaternary and Tertiary deposits of the map area. The high ridges and deep valleys characteristic of parts of the piedmont attest to the amount of stream erosion that has occurred since the highest levels of alluvium were deposited. Episodes of downcutting of Pantano Wash caused erosion of the toes of alluvial fans on both sides of the valley, and resulted in much of the stream downcutting in the piedmonts adjacent to the creek. Streams that head in the mountains flow across the piedmonts and eventually join Pantano Wash. The lower ends of these streams are linked with the creek, so episodes of downcutting in Pantano Wash tend to steepen and downcut the slopes of its tributary stream channels as well. The ultimate cause of the downcutting by the larger streams in southeastern Arizona is not certain. It is may have occurred a delayed response of the integration of the Tucson basin streams into the larger regional drainage system. The oscillating climatic conditions of the Quaternary may have resulted in higher long-term erosion rates than during the Miocene and Pliocene [Peizhen and others, 2000]. Alternatively, the downcutting may have been driven by some broad regional upwarping of southeastern Arizona, the cause of which is not known [Menges and Pearthree, 1989].

The fact that we observe suites of alluvial surfaces with similar characteristics and topographic relationships throughout southern Arizona implies that the factors that are controlling erosion and deposition in fluvial systems are regional in scope. Whether fluvial systems aggrade or degrade is a function of sediment supply and their ability to transport sediment. Most of the area within drainage systems consists of hillslopes, where sediment is generated from weathering of bedrock and in turn is weathered in place and/or transported downslope to the stream system. If hillslopes are stable, then weathering dominates and sediment supply to streams is relatively low. These conditions probably existed in this region during glacial intervals, when vegetation density on hillslopes was greater due to increased annual precipitation and/or decreased summer temperatures in this region. Hillslopes have probably been unstable during changes between glacial and interglacial conditions, as vegetation responded to changing climate and the character of precipitation and runoff varied in response to changes in the nature and frequency of thunderstorm activity. Because of these climate-induced changes, large fluxes of sediment may have been introduced into the fluvial systems, causing periods of aggradation on the piedmont. The fans and terraces of the map area likely record climate changes of this kind.

The most recent cycle of stream downcutting within the larger drainage basin began in the late 1800's and is probably continuing now. Historical photographs indicate that the floodplain of Cienega Creek at Pantano site (just east of the map area) was unentrenched with no obvious channel in early 1880 [Myrick, 1975; Dobyns, 1981]. Within 10 years, however, a large, deep channel had developed in this area, causing the railroad track to be relocated to higher ground. Remnants of the early historical floodplain in this area today are about 5 m above the modern channel and support a lush stand of mesquite trees. It is likely that arroyo development proceeded upstream rapidly in the subsequent large floods of the late 1800's and early 1900's. Currently, Cienega Creek is deeply entrenched below its historical floodplain throughout the Cienega Gap area. Tributary streams are also entrenched near their confluences with Cienega Creek, but entrenchment on even the largest tributaries such as Davidson Creek decreases quite rapidly upstream.

Geologic Hazards

This section summarizes the character and distribution of the principal geologic hazards that exist in and around the map area. This information is general in nature. Detailed site-specific geologic, engineering, hydrologic, or soils investigations may be required to thoroughly assess potential hazards at particular locations. More specific information on soil properties may be obtained from the USDA Natural Resources Conservation Service, and information on mapped floodplain and flood-prone areas may be obtained from the Pima County Flood Control District.

Flood hazards. Hazards related to flooding in the map area may be subdivided into two broad categories. Along the main drainages and their tributaries, flood hazards consist mainly of channel and floodplain inundation and lateral erosion of unprotected channel banks. The most widespread flood hazards are those associated with smaller tributary drainages on piedmonts, where the extent of flood-prone area varies with the size of the stream and local topographic confinement of floodwater. This latter category of flood hazard is particularly difficult to assess in areas where channel networks are distributary and topographic relief is low. These areas may be subject to alluvial fan flooding.

Records from three USGS stream gages on Pantano Wash are available. One gage (Pantano Wash near Vail) is just downstream from the confluence of Aqua Verde and Cienega creeks and has records from 1959. A second gage (Pantano Wash near Tucson) was located at Tanque Verde Road and recorded flow from 1935 to 1985. The third gage (Pantano Wash at Broadway) has records from 1978. Moderate to large floods on Pantano Wash occurred in 1940, 1958, 1959, 1963, 1964, 1971, 1981,and 1983. In August 1958, a discharge of 38,000 cubic feet per second (cfs) was estimated at the Pantano Wash near Vail gage [Pope and others, 1998; U.S. Geological Survey, 2001]. In fact, the estimated peak discharge for this flood is 3 times larger than any other flood of the gage record. All of the sizable floods on Pantano Wash have occurred in August, September, or early October. This suggests that exceptional summer monsoon storms and occasional dissipating tropical storms generate the floods on this small regional drainage.

Prior to the gage record, large summer floods on Cienega Creek in the 1880's and 1891 began the development of the modern entrenched arroyo system [Myrick, 1975]. The channels of Cienega Creek, and Davidson Creek from its confluence with Cienega Creek south to I-10, are entrenched one to 5 meters below the floodplain of the middle 1800's. The capacity of the channels and low overbank areas is generally sufficient to convey flood discharges through this area without inundating former floodplain areas that are now terraces. Lateral bank erosion, however, is certainly a significant hazard as hundreds of feet of erosion may occur during floods (for example, Parker, 1995; Wood and others, 1999]. The potential for serious bank erosion exists along extensive, unprotected banks formed in weakly consolidated Qy_{2r} and Qy_{ra} deposits.

Smaller tributaries that drain the mountain ranges and the piedmonts are subject to flash floods. Floods on these drainages result from intense, localized thunderstorms that occur during the summer or early autumn, and stream stages typically rise and fall rapidly during floods. Flood hazards are relatively easy to manage where topographic relief contains floodwater to channels and adjacent low terraces. In these situations, the area that may be impacted by flooding is limited and should be easy to avoid. It is much more difficult to assess and manage flood hazards associated with alluvial fan flooding. This type of flooding occurs where topographic relief is minimal and floodwater can spread widely. In these areas, channels may or may not be well defined, and their positions may shift during floods, and inundation is likely to be widespread during floods.

Surficial geologic mapping provides important information about the extent of flood-prone areas on the piedmonts, and it is the best way to delineate areas that may be prone to alluvial fan flooding. Floods leave behind physical evidence of their occurrence in the form of deposits. Therefore, the extent of young deposits on piedmonts is a good indicator of areas that have been flooded in the past few thousand years. These areas are most likely to experience flooding in the future. Following this logic, the extent of potentially flood-prone areas on the piedmont varies with the extent of young deposits (units Qy_2, Qy_1, and Qy). Active alluvial fans may be recognized by both distributary (downstream-branching) channel networks and laterally extensive young deposits between channels (see Pearthree and others, 1992].

Most of the modern drainages on the piedmonts have tributary networks that are topographically confined by ridges of older alluvium. Along these drainages, flood hazards are restricted to active channels and adjacent low, young terraces (unit Qy_2 or Qy). Portions of the slightly older and higher terraces that are mapped as unit Qy_1 may be subject to rare inundation in extreme floods. There are some distributary drainage systems on the lower piedmont areas, especially in the northwestern portion of the map area, that are subject to broad sheetflooding and possibly alluvial-fan flooding. Flood hazards are greatest at the upslope end of these areas, at the transition from confined to unconfined flow, because of fairly deep flow, high flow velocities, and the potential for significant changes in channel position during floods. Unconfined flow during floods occurs along floodplain margins of major drainages where tributaries debouch from the topographically confined foothills onto Qy_{1r} or Qy_1 terraces.

Soil problems. Soils in the Tucson area present a number of problems to homeowners. Cracking of foundations, walls, driveways, and swimming pools causes headaches and costs millions of dollars each year in repairs. Severe or recurring damage can lower the value of a house or commercial property. Leading in the list of potential soil properties that can cause structural failures are expansive soils and collapsing soils. Properties of problem soils are generally related to the type and amount of clay, and to the conditions under which the clay originated. Clay minerals can form in-place by weathering of rocks, or by deposition from water or wind.

Potential soil problems in middle and upper piedmont areas consist of shrink-swell potential, low infiltration rates, and hard substrate. Shrink-swell problems may exist on clay-rich soils of unit Qm and Qmo, although the gravel that is common in these deposits may minimize these problems. Excavation may be difficult and near-surface infiltration rates low on the oldest piedmont units (Qmo and QTs) due to the existence of carbonate- and silica-cemented hardpans (petrocalcic and duric horizons). Excavation and infiltration problems may be encountered on all surficial units in the uppermost piedmont areas because of the existence of bedrock at shallow depths.

Land subsidence and earth fissures. In the Tucson area, agricultural development and population increases have resulted in the heavy use of groundwater resources. Because groundwater recharge in the area is limited, groundwater levels have been lowered up to several hundred feet in parts of the Tucson area. Earth fissures have developed in Avra Valley, and recent measurements have indicated that the surface of the central part of the Tucson basin (northeast of the map area) has begun to subside.

Withdrawal of groundwater at rates faster than natural recharge leads to declines in water tables. Water levels in parts of Tucson's central well field had declined by more than 150 feet by 1981 [Anderson, 1988] and are continuing to decline. Water levels have declined by 50 to 150 ft in most of Avra Valley, but levels may not be declining in that area at present [Anderson, 1989]. Dewatering of sediments causes compaction, which in turn results in lowering of the land surface. In every Arizona groundwater basin where groundwater overdraft has occurred, subsidence has followed. Land subsidence is as much as 15.4 feet near Eloy [Slaff, 1993] and 18 feet west of Phoenix [Schumann, 1992]. In the Tucson basin, subsidence was detected in re-leveling surveys in 1952 [Platt, 1963], but maximum total subsidence was only about 0.5 feet by 1980 [Anderson, 1988].

Recent surveys have indicated continuing subsidence as water levels decline under Tucson. Hatch [1991] measured an average subsidence rate of 1 cm per year over the Tucson basin from 1987 to 1991. Based on the amount and rate of past subsidence, parts of the Tucson basin can expect subsidence of more than 10 feet by the year 2030 [Anderson, 1988]. In Avra Valley, 10 ft or more of subsidence is possible in the northern part of the basin if water levels continue to decline [Anderson, 1989]. Measurements in the Tucson basin suggest that the rate of subsidence has increased markedly since 1980. Confirmation of the increased rate of subsidence is provided by a preliminary survey of subsidence using satellite-based synthetic aperture radar interferometry. Using SAR interferometry, a British company measured 9 cm of subsidence over a 3 year, 9 month period, ending in March, 1997, yielding a rate of 2.4 cm/yr [Galloway and others, 1999].

In Arizona basins where subsidence is more than a few feet, earth fissures have developed. A fissure developed in northern Avra Valley east of Marana High School adjacent to the Central Arizona Project aqueduct [Arizona Geological Survey, 1988]. It was quickly filled and surface water was diverted from it, and it has not reopened. The Tucson basin is the only one of Arizona's deep groundwater basins where groundwater level declines and land subsidence have not yet been followed by earth fissures, probably because the amount of total subsidence has thus far been relatively small compared to other basins. With the expected lowering of water tables and subsequent predicted land subsidence, earth fissures may be expected to develop in Tucson as they have elsewhere.

Earthquake hazards. There has been very little historical seismic activity in southeastern Arizona with the exception of the Sonoran earthquake on May 3, 1887. This magnitude ~7 ¼ event, centered southeast of Douglas, Arizona, caused strong shaking and damage throughout southeastern Arizona. Later that year, at least two earthquakes were reported from observers on the railroad in the Pantano area [DuBois and others, 1982]. Based on the location of the maximum shaking reported for these events, they were likely located in or near Cienega Gap. No subsequent seismic activity has been reported for this area.

The map area is in close proximity to the northern end of the Santa Rita fault zone, which extends along the Santa Rita Mountains for about 35 miles (60 km) from Tubac to just northeast of Corona de Tucson [Pearthree and Calvo, 1987]. Along the fault zone, a discontinuous zone of fault scarps offset Pleistocene alluvium. Scarps trend northeast to north-south and are 1 to 6 km west of the base of the Santa Rita Mountains. Scarps range up to about 5 m in height and have maximum slope angles up to about 10°. Surficial deposits as young as late Pleistocene are displaced but latest Pleistocene and Holocene deposits are not faulted, which brackets the age of youngest faulting between 10-20 ka and 75-130 ka. Quantitative analysis of fault scarp morphologies indicates that the youngest surface rupture occurred between about 60-130 ka. Fault displacement of late Pleistocene surfaces averages about 2 m, in contrast to 4 to 5 m of displacement of middle and early Pleistocene surfaces. Using surface displacement estimates and various estimates of surface rupture length, Pearthree and Calvo [1987] concluded that two paleoearthquakes of magnitude 6 ¾ to 7 ¼ occurred along the Santa Rita fault zone in the past 200 to 300 ka. Geophysical investigations on the northern part of the fault zone indicate that that part of the fault dips shallowly to the northwest [Johnson and Loy, 1992]. This implies that the area of the seismogenic fault may be larger than previously suspected, and that it dips beneath the Tucson metropolitan area.

The evidence of low frequency Quaternary fault activity combined with the existence of broad bedrock pediments on the west side of the Santa Rita Mountains indicates that the long-term slip rate on the Santa Rita fault zone is very low. The very long recurrence intervals between surface ruptures and evidence for very low long-term slip rates are consistent with other Quaternary fault zones that have been studied in southeastern Arizona, southwestern New Mexico, and northern Sonora [Pearthree, 1986; Bull and Pearthree, 1988; Demsey and Pearthree, 1994; Pearthree, 1998]. The fault activity that is observed in this region is either a late pulse of activity related to the Basin and Range disturbance or a new, weakly extensional tectonic regime that has developed in the middle to late Quaternary.

STRUCTURAL GEOLOGY

Complexly deformed Tertiary and older strata in the study area are in the hanging wall of the Catalina detachment fault. This major regional fault crops out east and northeast of the Vail quadrangle. The crystalline rocks of the Rincon Mountains form the southern end of the Catalina metamorphic core complex [Drewes, 1977; Davis, 1980; Banks, 1980; Keith et al., 1980; Dickinson, 1991; Force, 1997]. The Catalina detachment fault is a gently to moderately southwest-dipping normal fault with at least 27 km of displacement [Dickinson, 1991]. This displacement uncovered the mid-crustal gneissic and granitic rocks that form the Rincon Mountains.

Paleozoic to middle Proterozoic strata and middle Proterozoic diabase in the Colossal Cave area are complexly and multiply folded and faulted. Some strata are overturned. These rocks record a complex history of deformation before deposition of the Pantano Formation in Oligocene time.

Pre-Cretaceous uplift of rocks in the northern Empire Mountains is inferred to have caused erosional removal of all strata above Proterozoic granite that was then buried by the late Jurassic to early Cretaceous Glance conglomerate and younger strata [Bilodeau, 1979]. This uplift event is not well understood. The southern boundary of this middle Mesozoic uplift is located in the Empire Mountains, south of the map area [Spencer et al., 2002], where an east-west trending belt of complex faulting juxtaposes granitoids and Pinal Schist against Paleozoic and Mesozoic strata to the south. Finnell [1971] interpreted this as a zone of north-dipping thrust faults. Such thrust or reverse faulting could have caused uplift of the northern, hanging-wall block. Bilodeau [1979] and Bilodeau et al. [1987] inferred that movement on south-dipping normal faults caused uplift of the northern, footwall block, and that later reverse faulting occurred along or near the normal fault zone, obscuring the older normal faults. The fault zone is exposed in and area of low relief, and contacts are generally concealed to a degree that does not allow ready determination of the nature or dip of the possible or known fault contacts [Spencer et al., 2002]. At one location (NE ¼, SW ¼, sec. 14, T. 17 S., R. 17 E.), a fault in this fault zone dips 45° to the northwest and places Proterozoic Pinal Schist over a sliver of Paleozoic carbonate that is bounded to the southeast by Proterozoic granite. The carbonate sliver suggests that the fault has had a complex movement history, possibly involving both normal and reverse faulting [Spencer et al., 2002].

The northern boundary of the middle Mesozoic uplift lies in the southeastern part of the map area shown in Plate 1. Strata of the Bisbee Formation are deposited on Proterozoic granitoid in the southeastern corner of the map. Upper Paleozoic strata, with locally preserved, probable pre-Bisbee lower Mesozoic strata (unit JTRlv, JTRgs, JTRgm), form a generally west-southwest dipping homocline along the ridges south of Colossal Cave in the central eastern part of the map. These outcrop areas are separated by about 2 km of Tertiary cover, requiring either a dramatic angular unconformity or fault between them.

Almost all of the Tertiary strata in the map area are included in the Pantano Formation [Brennan, 1962; Finnell, 1970]. The lower part of the Pantano Formation consists of faulted and tilted conglomerate, sandstone, siltstone, and clay, with interbedded volcanic unit that is ~27 Ma in age. The degree of tilting and faulting in the Pantano Formation decreases dramatically up-section within the fine grained upper part. In the Rincon Peak and The Narrows quadrangles to the east of the map are, the overlying breccia facies, Conglomerate of Agua Verde Creek, and Unit of Wakefield Canyon are typically only slightly faulted and deformed [Spencer et al., 2002]. Only one small outcrop area of the Conglomerate of Agua Verde Creek is recognized in the map area, and is characterized by debris that appears to have been derived from leucocratic and mylonitic granitoids in the Rincon Mountains. Strata of the Conglomerate of Agua Verde Creek in the map area are gently to moderately tilted.

MINERAL DEPOSITS

Barite deposits in the Colossal Cave area consist of 1-3 m thick, irregular, elongate masses hosted by Mississippian Escabrosa Limestone (NE ¼, NE ¼, sec. 8, T. 16 S., R. 17 E.). Barite is massive, white, with no other identified hydrothermal minerals. Small prospect pits are located on some deposits.

A 30-cm-thick quartz-calcite-specular hematite vein is exposed in a prospect pit near Agua Verde Creek (NW ¼, NE ¼, sec. 17, T. 16 S., R. 17 E.; Vail 7 ½' Quadrangle).

A series of prospects along the fault between Paleozoic strata and Proterozoic granodiorite (UTM 530418E, 3545250N) has apparently been obliterated by recent bulldozing. Float in the area includes abundant milky vein quartz and brecciated vein quartz cemented by red earthy hematite. Some vein quartz contains drusy quartz crystals in vugs filled with red earthy hematite. Sparse green secondary copper oxide mineralization (malachite?) was observed in some of these vugs, and along fractures in the rock. A calcite replacement vein is present in crushed Xgd along the fault against the Paleozoic strata. Xgd is moderately to strongly chloritized and silicified in a 20 m thick zone of strong fracturing adjacent to the fault. A mafic dike in this zone intrudes altered rock and is not silicified (too small to show on map).

Silicification

In the vicinity of Colossal Cave a variety of rock ranging from Proterozoic granodiorite to conglomerate of the Pantano Formation are variably silicified. Where the silicification is weak, the rock is simply more indurated than non-altered equivalents. Advanced alteration results in complete replacement of the rock by silica, accompanied by introduction of iron oxide to the rock. The resulting rock is a massive jasperoid (Unit Tsx). This style of alteration resembles that described in association with sediment-hosted disseminated gold deposits [Fournier, 1985; Percival et al., 1988]. Alteration of Pantano Formation conglomerate indicates that the silicification is Tertiary in age. If the alteration cut by the mafic dike at the prospect mentioned above were related to the silicification, as would appear to be the case, then the alteration occurred before cessation of igneous activity in the area. The youngest dated igneous rocks in the adjacent areas are late Oligocene in age (see Unit Ta, below). These observations suggest that the alteration is Tertiary in age, and occurred early in the development of the Catalina Core complex.

Fournier [1985] suggests three mechanisms for silica-replacement of rock to form jasperoid in carbonate rocks. These include 1) slow cooling of near-neutral pH aqueous fluid; 2) reaction of silica-rich acidic aqueous fluid with limestone; and 3) reaction of strongly oxidized fluid with organic matter in limestone to reduce the oxidation. In the Colossal Cave area, both limestone and quartzo-feldspathic rocks are replaced by silica. Associated argillic alteration indicative of strong acid alteration is absent in rocks adjacent to the silicified zone. These observations argue against the role of strongly acidic solutions in the silicification. Silicification of granitic rocks strongly indicates that reduction of oxidized fluids by organic matter in the limestone was not an essential aspect of the alteration. Thus, the most likely process involved cooling of near-neutral pH aqueous fluids. Because such fluid will dissolve limestone as silica is precipitated, replacement of the limestone is easily understood. The replacement of Pantano conglomerate and Proterozoic granite by silica is more problematic, because it requires removal of alkalis and alumina. The geochemistry of this reaction is not presently understood.

Formation of large jasperoid bodies is not typical of hydrothermal systems associated with middle-Tertiary extension and low-angle normal faulting in the region [Liebler, 1988; Wilkinson et al., 1988; Spencer and Welty, 1989]. Significant hematite replacement bodies are reported from the Buckskin Mountains [Spencer and Welty, 1989], and silicified breccias are associated with faults in the Riverside Mountains [Wilkinson et al., 1988]. The Colossal Cave area-silicified zones are also distinctive in their lack of metallic mineralization. The location, structural setting, and age of silicification in the Colossal Cave area, along with the absence of an associated magmatic source strongly suggests a relationship to detachment faulting similar to that proposed in these other examples. Further study of this alteration and comparison to alteration associated with other detachment-related mineralization may help elucidate the chemistry and dynamics of hydrothermal systems associated with detachment faults.

ROCK UNITS

Quaternary and Late Tertiary map units

d **Disturbed ground (<100 years)—**Areas where human activity has obscured the geologic nature of underlying material. Generally non-consolidated, very poorly sorted mud, sand, and gravel, with variable amounts of pavement.

Qs **Surficial deposits, undivided (Quaternary).**

Piedmont Alluvium

Quaternary and late Tertiary deposits cover most of the piedmont areas, and extend onto older deposits of the Tucson Basin. This alluvium was deposited primarily by larger streams that head in the mountains. Smaller streams that head on the piedmont have eroded and reworked some of these deposits. Surficial deposits range in age from modern to early Pleistocene, with some older basin fill deposits extending to the Miocene. Approximate age estimates for the various units are given in parentheses after the unit name. Abbreviations are ka, thousands of years before present, and Ma, millions of years before present.

Qy_2 **Late Holocene alluvium (<2 ka).** Unit Qy_2 consists of channels, low terraces, and small alluvial fans composed of cobbles, sand, silt and boulders that have been recently deposited by modern drainages. In upper piedmont areas, channel sediment is generally sand, pebbles and cobbles, with some boulders; terraces typically are mantled with sand and finer sediment. On lower piedmont areas, young deposits consist predominantly of sand and silt, and some cobbles in channels. Channels generally are incised less than 1 m below adjacent terraces and fans, but locally incision may be as much as 2 m. Channel morphologies generally consist of a single-thread high flow channel or multi-threaded low flow channels with gravel bars adjacent to low flow channels. Downstream-branching distributary channel patterns are associated with the few young alluvial fans in the area. In these areas, channels typically are discontinuous, with small, well-defined channels alternating with broad expansion reach where channels are very small and poorly defined. Local relief varies from fairly smooth channel bottoms to the undulating bar-and-swale topography that is characteristic of coarser deposits. Terrace typically have planar surfaces, but small channels are also common on terraces. Soil development associated with Qy_2 deposits is minimal. Terrace and fan surfaces are brown, and on aerial photos they generally appear darker than surrounding areas, whereas sandy to gravelly channels appear light-colored on aerial photos. Vegetation density is variable. Channels typically have sparse, small vegetation. Along the larger washes, vegetation includes mesquite, yuccas, acacias; smaller bushes and grass may also be quite dense. Smaller washes typically have palo verde, mesquite, large creosote and other bushes along them.

Qy_1 **Holocene alluvium (~2 to 10 ka).** Unit Qy_1 consists of low terraces found at scattered locations along incised drainages and broad, minimally dissected alluvial fans. Qy_1 surfaces are slightly higher and less subject to inundation than adjacent Qy_2 surfaces. Surfaces are generally planar; local relief may be up to 1 m where gravel bars are present, but typically is much less. Qy_1 surfaces are less than 2 m above adjacent active channels. Surfaces typically are sandy but locally have fine, unvarnished open gravel lags. Qy_1 surfaces generally appear fairly dark on aerial photos, but where a gravel lag is present, surfaces are light colored. Channel patterns on alluvial fans are weakly integrated distributary (branching downstream) systems. Qy_1 soils typically are weakly developed, with some soil structure but little clay and stage I to II calcium carbonate accumulation (see Machette, 1985, for description of stages of calcium carbonate accumulation in soils). Qy_1 terrace surfaces support mesquite, prickly pear, yucca, and smaller bushes. Qy_1 fans support scattered trees along channels, but creosote and other small bushes are dominant.

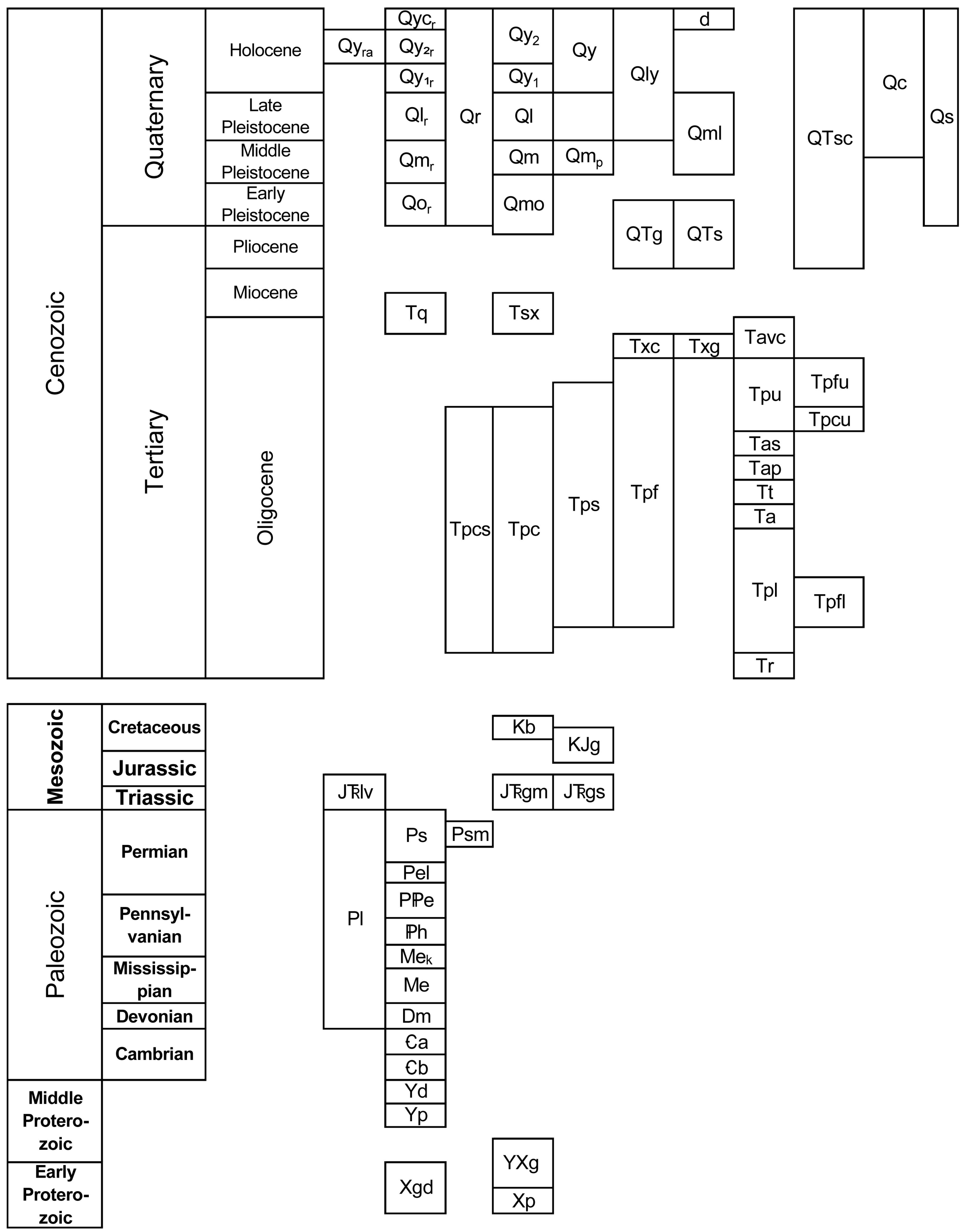

Figure 1. Correlation of Map Units.

Qy **Undifferentiated Holocene alluvium (< 10 ka)** Unit Qy includes both Qy_2 and Qy_1 deposits. It is used where it was not possible, at a scale of 1:24000, to separately map Qy_1 and Qy_2 surfaces. Unit Qy consists of smaller incised drainages on the piedmont and more extensive young alluvial fans at the base of the piedmonts. Soil development consists of cambic horizons over weak to moderate (stage I to II) calcic horizons.

Qly **Holocene to late Pleistocene alluvium (0 to 130 ka).** Broadly rounded alluvial fan surfaces approximately 1 m above active channels composed of mixed alluvium of late Pleistocene and Holocene age. Drainage networks consist of a mix of distributary channel networks associated with larger drainages and tributary channels associated with smaller drainages that head on Qly surfaces. Qly areas are primarily covered by a thin veneer of Holocene fine-grained alluvium (unit Qy), but reddened Pleistocene alluvium (unit Ql and rarely, Qm) is exposed in patches on low ridges, in roads, and in cut banks of washes. The Holocene surfaces usually are light brown in color and soils have weak subangular blocky structure and minor carbonate accumulation. Qly fans mainly support creosote bushes.

Ql **Late Pleistocene alluvium (~10 to 130 ka).** Unit Ql consists of slightly to moderately dissected relict alluvial fans and terraces found on the upper, middle and lower piedmont, and scattered within the mountains. Moderately to well-developed, slightly to moderately incised tributary drainage networks are typical on Ql surfaces. Active channels are incised up to about 2 m below Ql surfaces, with incision typically increasing toward the mountain front. Ql fans and terraces are commonly lower in elevation than adjacent Qm and older surfaces, but the lower margins of Ql deposits lap out onto more dissected Qm surfaces in some places. Ql deposits consist of pebbles, cobbles, and finer-grained sediment. Ql surfaces commonly have loose, open lags of pebbles and cobbles; surface clasts exhibit weak rock varnish. Ql surfaces appear light orange to dark orange on color aerial photos, reflecting slight reddening of surface clasts and the surface soil horizon. Ql soils are moderately developed, with orange to reddish brown clay loam to light clay argillic horizons and stage II calcium carbonate accumulation. Dominant forms of vegetation include grasses, small shrubs, and mesquite. Ql fans derived from carbonate-rich sources typically are gray on aerial photographs, have stage II-III calcium carbonate accumulation, and have dense and very diverse vegetation, such as palo verde and mesquite trees, several species of shrubs and cacti, but very few annuals.

Qml **Middle to late Pleistocene alluvium (~10 to 500 ka).** Unit Qml consists of mixed hillslope colluvium and middle to late Pleistocene alluvium that has formed as valley fill along drainages in unit QTs. Deposits range in thickness and soil development.

Qm **Middle Pleistocene alluvium (~130 to 500 ka).** Unit Qm consists of moderately dissected relict alluvial fans and terraces with strong soil development found throughout the map area. Qm alluvium is deposited on top of unit QTs, which is often exposed beneath. Qm surfaces are drained by well-developed, moderately to deeply incised tributary channel networks; channels are typically several meters below adjacent Qm surfaces. Well-preserved, planar Qm surfaces are smooth with moderate to tightly packed pebble and cobble lags; surface color is reddish brown; rock varnish on surface clasts is typically orange or dark brown. More eroded, rounded Qm surfaces are characterized by scattered cobble lags with moderate to strong varnish, broad ridge-like topography and some carbonate litter on the surface. Well-preserved Qm surfaces have a distinctive dark orange color on color aerial photos, reflecting reddening of the surface soil and surface clasts. Soils typically contain reddened, clay argillic horizons, with obvious clay skins and subangular to angular blocky structure. Underlying soil carbonate development is typically stage III, with abundant carbonate through at least 1 m of the soil profile; indurated petrocalcic horizons are rare. Qm surfaces generally support grasses, mesquite, palo verde, yuccas, shrubs and ocotillo.

Qm_p **Middle Pleistocene alluvium over dissected pediment (~130 to 500 ka).** Unit Qm_p consists of thin, discontinuous deposits of Qm over dissected pediment, or on as remnant terrace and fan deposits over bedrock on the piedmonts north of Pistol Hill.

Qmo **Middle to early Pleistocene alluvium (~500 ka to 2 Ma).** Unit Qmo consists of very old, high, dissected alluvial fan remnants with moderately well preserved fan surfaces and strong soil development. Qmo surfaces typically are fairly smooth to broadly rounded. Qmo alluvium is deposited on top of unit QTs, which is often exposed on hillslopes beneath Qmo. Qmo deposits consist of cobbles, gravels and boulders, with sand and finer clasts. Well-preserved, planar Qmo surfaces are smooth with moderate to tightly packed cobble and boulder lags; surface color is dark red; rock varnish on surface clasts is strong and typically orange or dark brown. Qmo soils are dark red with well-developed, heavy clay argillic horizons. Stage III to IV calcic horizons are typical. Qmo surfaces are dominated by grass, mesquite, prickly pear, cholla, and ocotillo.

QTs **Early Pleistocene to late Miocene alluvium (~1 to 10 Ma).** Unit QTs consists of very old, deeply dissected and highly eroded alluvial fan deposits. QTs surfaces vary from highly eroded ridges and deep valleys, with ridgecrests typically 10 to 30 meters above adjacent active channels, near the mountains to broadly rounded ridges towards Cienega Creek. The thickness of QTs deposits is not known. They are drained by deeply incised tributary channel networks. Even the highest surfaces atop QTs ridges are rounded, and original highest capping fan surfaces are not preserved. QTs deposits are dominated by gravel ranging from boulders to pebbles. Deposits are moderately to very strongly indurated and are quite resistant to erosion because of the large clast size and carbonate cementation. Soils typically are dominated by carbonate accumulation, which is typically stage V (cemented petrocalcic horizons with laminar cap) on ridgecrests. Carbonate litter is common on ridgecrests and hillslopes. On aerial photos, QTs surfaces are gray to white. QTs surfaces support creosote, mesquite, palo verde, ocotillo, and cholla.

QTso **Mapped exposures of QTs deposits** beneath colluvium.

QTg **Early Pleistocene to late Miocene gravel or conglomerate (1 to 10 Ma).** Unit QTg is very similar to unit QTs in landscape placement and morphology. QTg deposits are coarser than QTs deposits and are dominated by boulders and cobbles. The thickness of QTg deposits is not known. Deposits are moderately to very strongly indurated and are quite resistant to erosion because of the large clast size and carbonate cementation. Soils typically are dominated by carbonate accumulation, which is typically stage V (cemented petrocalcic horizons with laminar cap) on ridgecrests. Carbonate litter is common on ridgecrests and hillslopes. On aerial photos, QTg surfaces are gray to white. QTg surfaces support creosote, mesquite, palo verde, ocotillo, and cholla.

QTsc **Pantano Formation and hillslope deposits mantling Pantano Formation, undivided (Quaternary to late Tertiary)—**Deposits of this unit include very old, deeply dissected and highly eroded alluvial fan deposits and underlying Pantano Formation in areas where the Pantano Formation has not been divided from younger deposits. QTsc surfaces are alternating eroded ridges and deep valleys, with ridgecrests typically 10 to 30 meters above adjacent active channels. The thickness of QTsc deposits is not known. QTsc surfaces are drained by deeply incised tributary channel networks. Even the highest surfaces atop QTsc ridges are rounded, and original highest capping fan surfaces are not preserved. QTsc deposits are dominated by gravel ranging from boulders to pebbles. Deposits are moderately indurated and are quite resistant to erosion because of the large clast size and carbonate cementation. Also included are areas where incision is moderate to slight, underlying Pantano Formation is fine grained and poorly resistant, and unit QTsc has been outlined by aerial photograph analysis of low relief areas where a large amount of fine grained Pantano Formation is apparent by its very light shades but a veneer of remobilized Pantano Formation and other Quaternary deposits is also apparent. Soils typically are dominated by carbonate accumulation, which is typically cemented on ridgecrests. Carbonate litter is common on ridgecrests and hillslopes. On aerial photos, QTsc surfaces are gray to white. QTsc surfaces support creosote, mesquite, palo verde, ocotillo, and cholla.

Axial Stream Deposits

Sediment deposited by Cienega and Davidson creeks and Pantano Wash are mapped separately. The name Pantano Wash is used for the stream below the confluence of Cienega and Agua Verde creeks. Deposits are a mix of gravel, sand and finer material; older deposits are coarser than younger deposits; they exhibit mixed clast types and a higher degree of rounding reflecting the large drainage areas of these streams.

Qr **Undifferentiated river terraces (Quaternary).**

Qyc_r **Late Holocene channel deposits (< 100 years).** This unit consists of river channel deposits. Deposits are composed primarily of sand and gravel. The modern channels are typically entrenched several meters below adjacent young terraces. The current entrenched channel configuration began to evolve with the development of arroyos in the late 1800's, and continued to evolve through this century [Myrick, 1975; Dobyns, 1981]. Channels are extremely flood prone and are subject to deep, high velocity flow in moderate to large floods. Most modern channel banks are formed in weakly to moderately cohesive late Holocene alluvium and may be subject to severe lateral erosion during floods. Erosion is likely to be most severe on the outside banks of channel bends.

Qy_{2r} **Late Holocene river alluvium (<150 years).** Unit Qy_{2r} consists of modern floodplains and low terraces deposited along modern channels since the entrenchment of the 1800's. Qy_{2r} deposits are composed primarily of sand and finer-grained material. Qy_{2r} surfaces will be inundated in large floods. Terraces typically have planar surfaces, but small channels are also common on terraces. Soil development associated with Qy_{2r} deposits is minimal. Unprotected channel banks formed in Qy_{2r} deposits are very susceptible to lateral erosion. .

Qy_{ra} **Recently abandoned late Holocene floodplain and terrace deposits (< 2 ka).** Unit Qy_{ra} are remnant terraces abandoned between 1880 and 1887 when several washouts along the railroad track occurred [Myrick,1975; Dobyns, 1981]. Qy_{ra} deposits are composed of very fine silt and sand deposits incised 3 to 5 meters above the active channels. These terraces are covered with thick mequite bosques. They are found only along Cienega and Davidson creeks, and uppermost Pantano Wash.

Qy_{1r} **Holocene river terrace deposits (2 to 10 ka).** Unit Qy_{1r} consists of moderately low terraces flanking the main channel of Pantano Wash, and abandoned terraces along Cienega and Davidson creeks. Terrace surfaces are flat and relatively uneroded, except where immediately adjacent to modern channels. Qy_{1r} deposits consist of weakly to unconsolidated sand, silt, and clay. Soils are weakly developed, with some carbonate filaments and fine masses and weak soil structure in near surface horizons. Along Pantano Wash, Qy_{1r} surfaces may experience sheetflooding during large floods in areas where the main channel is not deeply entrenched, and as a result of flooding on local tributaries that debouch onto Qy_{1r} surfaces.

Qlr **Late Pleistocene river terrace deposits (~10 to 130 ka).** Unit Qlr consists of remnant river terrace deposits along Cienega and Davidson creeks and Pantano Wash. These terraces are typically 10 m above the active channel Cienega and Davidson creeks to 5 m along Pantano Wash. Qlr deposits consist of cobbles, gravels and finer-grained sediment. Qlr surfaces commonly have loose, open lags of cobbles and gravels; surface clasts exhibit weak rock varnish. Qlr surfaces appear light orange color aerial photos, reflecting slight reddening of surface clasts and the surface soil horizon. Qlr soils are moderately developed, with orange to reddish brown clay loam to light clay argillic horizons and stage II calcium carbonate accumulation. Vegetation on Qlr terraces consists of scattered mesquite, prickly pear and creosote bushes.

Qmr **Middle Pleistocene river terrace deposits (~130 to 500 ka).** Unit Qm_r consists of remnant river terrace deposits along Cienega and Davidson creeks and Pantano Wash. These terraces are typically 20 m above the active channel Cienega and Davidson creeks to 10 m along Pantano Wash. Qmr deposits consist of cobbles, gravels and finer-grained sediment. Qmr surfaces commonly have loose, open to moderately packed cobbles and gravel surface lags; surface clasts exhibit moderate rock varnish. Qmr surfaces appear in orange color aerial photos, reflecting reddening of surface clasts and the surface soil horizon. Soils typically contain reddened, clay argillic horizons, with obvious clay skins and subangular to angular blocky structure. Underlying soil carbonate development is typically stage III, with abundant carbonate through at least 1 m of the soil profile; indurated petrocalcic horizons are rare. Dominant vegetation includes mesquite and prickly pear cactus with fewer creosote bushes than Qlr terraces.

Qor **Early Pleistocene river terrace deposits (~1 to 2 Ma).** Unit Qor consists of ancient river terrace deposits along Cienega Creek and Pantano Wash. The tops of these terraces are 20 to 30 m above the active channel. Qor deposits consist of cobbles, pebbles, and a few small boulders with sand and finer-grained sediment. Qor surfaces commonly have a loose cobble and pebble lag; surface clasts exhibit moderate to strong rock varnish. Qor surfaces appear dark reddish brown in color aerial photos, reflecting reddening of surface clasts and the relatively clay-rich surface soil horizon. Soils typically contain reddish brown, clay argillic horizons. Soil carbonate development is strong, ranging from stage III to IV. Dominant vegetation includes mesquite, prickly pear cactus and creosote.

Hillslope Deposits

Qc **Hillslope colluvium (Holocene and Pleistocene).** Unit Qc consists of locally-derived deposits on moderately steep hillslopes in mountains. Colluvium is very extensive in the mountains, but is mapped only where sufficiently thick and extensive as to obscure underlying bedrock. Deposits are very poorly sorted, ranging from clay to cobbles and boulders. Clasts typically are subangular to angular because they have not been transported very far. Bedding is weak and dips are quite steep, reflecting the steep depositional environment. Deposits are a few meters thick or less; thickest deposits are found at the bases of hillslopes. Some stable hillslopes are covered primarily with Pleistocene deposits, which are typically reddened and enriched in clay. Other more active hillslopes are covered with Holocene deposits, which have minimal soil development.

Colluvium on east side of Pistol hill includes abundant boulders of Bolsa Quartzite. On the ridge northeast of Pistol Hill, the ridgecrest is a boulder lag deposit of 1-3 m diameter boulders of Bolsa Quartzite. Bedding varies erratically between boulders. These deposits are suspected to represent slumping of the quartzite onto non-resistant, poorly consolidated Conglomerate of Agua Verde Creek, which is in (reverse?) fault contact with the Paleozoic strata.

Tertiary map units

Tqv **Hydrothermal silica and quartz – hematite breccia (Oligocene or early Miocene)**—Fine grained to cryptocrystalline, hydrothermal quartz, brecciated quartz, quartz-hematite breccia, and local milky quartz that forms veins and irregular masses. Silica is locally vuggy with fine drusy quartz lining vugs. Quartz-hematite breccia consists of angular fragments of gray, fine grained to cryptocrystalline quartz with a reddish brown to brownish brick red, siliceous and hematitic matrix. Limestone host for hydrothermal silica and quartz is locally preserved as sheets and irregular masses within silica. Silica locally displays layers and laminations on weathered surfaces that are interpreted as reflecting relict layering in replaced carbonates, siliceous carbonates, and silty and sandy strata.

Crushed hydrothermal quartz and re-silicified hydrothermal quartz forms a discontinuous, ~1-3 m thick sheet along a low-angle fault contact that places upper Paleozoic carbonates over

Proterozoic rocks along the south side of Agua Verde Creek directly west of the Rincon Peak 7 ½' Quadrangle. Also, just west of Agua Verde 2 (Castle on the hill), in the Rincon Peak 7 ½' Quadrangle, a fault zone contains silica replacement and open space filling quartz. Some quartz is shattered and re-cemented with silica (SW ¼, NE ¼, sec. 17, T. 16 S., R. 17 E.).

The vein that crops out on the hill labeled 'Isolated' (UTM 532290E, 3548565N) consists of banded milky microgranular quartz. This vein is 5-10 m thick. The western part of the vein has abundant interlayered brownish gray calcite.

Tsx **Jasperoid breccia, uncertain protolith (Oligocene or early Miocene)**—Massive red brown jasperoid. A wide variety of breccia textures are present, indicating multiple cycles of silicification and brecciation. Some clasts in the breccia may be relict from the original rock that was replaced by silica. Silicification has completely obliterated the identity of the protolith. In thin section, the rock is microgranular silica with disseminated tiny opaque (hematite?) grains. The texture of silica within fragments in the rock and in silica forming veins and cement between fragments is optically identical. Contacts with less silicified rock are generally gradational.

Tavc **Conglomerate of Agua Verde Creek (Oligocene to early Miocene)--** This conglomerate was named the Nogales Formation by Drewes [1977], presumably because he thought it was correlative with similar strata named the Nogales Formation near Nogales, Arizona [Simons, 1974], which is 60 km to the south. We do not think that the two are related, however, and consider this to be merely a basin-margin facies of strata deposited in the Pantano basin.

Conglomerate with sparse to abundant clasts of leucocratic granite, leucocratic muscovite granite, and variably lineated, mylonitic and locally chloritic granitoids, inferred to have been derived from the Rincon Mountains. This conglomerate is typically less indurated, lighter colored in general, and less tilted than conglomerate of the Pantano Formation. Crops out on west side of small basin between Colossal Cave and Pistol Hill. Apparently overlies conglomerate of Pantano Formation, but contact is not exposed.

Pantano Formation (Oligocene to Miocene)

The Pantano Formation was first described in detail by Brennan [1957, 1962], who designated and studied a type section along U.S. Highway 80 (now Interstate 10; see also Metz, 1963). Finnell [1970] identified several faults in Brennan's type section, described a revised stratigraphy consisting of five units, and elevated the formation name to formal status according to USGS guidelines. The lowest three of Finnell's five units are dominantly conglomeratic, the fourth consists of porphyritic andesite, and the fifth consists of conglomeratic sandstone grading upward into sandstone, siltstone, gypsiferous claystone, and breccia. Balcer [1984] mapped much of the Pantano Formation and re-defined its stratigraphy. He divided the breccia from Finnell's unit five to create a sixth, and highest, unit of breccia, and emphasized the calcareous and fine grained character of unit two. The combined thickness of Balcer's six units is 1277 m.

The fine grained siltstone and claystone of unit 5 of Balcer [1984] grade southeastward across discontinuous exposures into sandstone and conglomerate that are generally coarser grained toward bedrock exposures on the northeast flank of the Empire Mountains and toward the west flank of the Whetstone Mountains. This sandstone and conglomerate is here included with the Pantano Formation because it is interpreted as a basin-margin facies that formed as alluvial fans that flanked the playa deposits of unit 5.

Tpcs **Silicified conglomerate (Oligocene or early Miocene)--**Tan, strongly indurated conglomerate and conglomeratic sandstone of the Pantano Formation. Strongly cemented by silica, and cut by numerous silica veinlets. Rock fractures across clasts, and breaks into blocky outcrops. South and west of Colossal Cave hydrothermal silicification affects conglomerate and sandstone of map unit

Tdc, which indicates that silicification is Oligocene or younger. Near Agua Verde Creek rock avalanche breccia was derived from silicified quartzite, so silicification is older than youngest conglomerates of map unit Tdc. The hydrothermal quartz is thus interpreted to be Oligocene or early Miocene. This age assignment is based on the interpretation that hydrothermal silicification in the area was due to a single extensive event, rather than to smaller events separated by millions of year of time.

Undivided Pantano Formation

Tdf **Fine-grained siltstone and claystone, undivided.** Siltstone, silty clay, and clay, with local gypsum beds up to several cm thick. Color of clay is variable, and includes pale yellow, pale green, tan, and brown. Locally includes sandstone and sparse pebbly conglomerate. =

Tds **Sandstone.**

Tdc **Coarse-grained sandstone and conglomerate.** Massive to moderately well bedded, poorly sorted, pebble to boulder conglomerate. Locally includes sandstone and granule to pebbly sandstone. Clasts are mostly 3-30 cm and are locally as large as 2 m. Many smaller clasts are subangular, most others are subrounded. Colors are highly variable, and include tan, brown, and pale gray to greenish gray. Clasts compositions vary greatly over the area of exposure. Near Cienega Creek this unit contains abundant clasts of Bisbee Group sandstone and pale gray to whitish gray biotite quartz porphyry. Granitic clasts and clasts of limestone and quartzite are absent or rare. To the north near Agua Verde Creek, Paleozoic carbonate, quartzose sandstone clasts derived from the Cambrian Bolsa Quartzite, and granite or granodiorite derived from map unit YXg form most of the clasts. The absence of mylonitic clasts distinguishes this unit from the overlying Conglomerate of Agua Verde Creek.

Interbedded andesite of map unit Ta and tuff were dated by the K-Ar method at 24.9 ± 5.2 Ma (2σ uncertainty [95% confidence interval]) and 29.5 ± 1.8 Ma (2σ), respectively [Shafiqullah et al., 1978]. The andesite sample is from the large, irregular outcrop area along Cienega Creek west of Davidson Canyon, which probably is partly intrusive. The Location reported for the tuff sample was found to be conglomerate overlying the andesite. The tuff sample is probably from the Tdt outcrops about 680 m SE of the reported sample location. This tuff overlies the porphyritic andesite. These dates indicate that much or all of this conglomerate is Oligocene to early Miocene in age.

West and southwest of Colossal Cave, conglomerate, sandy conglomerate (50-90% conglomerate) and conglomeratic sandstone (50-90% sandstone), and local sandstone contain 2-30 cm clasts of quartz-phyric welded tuff similar to the rhyolite of Mt Fagan [Ferguson et al., 2002], Paleozoic carbonate and quartzite, and felsic granitic rocks but no mylonitic rocks. The conglomerate in this area becomes progressively more silicified to the north and grades into unit Tpcs.

Breccia facies, Pantano Formation

Txc Rock avalanche breccia derived from Paleozoic carbonate units (Oligocene to early Miocene). In canyon south of Colossal Cave visitor center, large blocks of Paleozoic carbonate strata occur in zone along contact with Davidson Canyon conglomerate. It is not clear if this is a mega breccia or disrupted, in place bedrock.

Txg Rock avalanche breccia derived from granitic rock (Oligocene to early Miocene). One breccia sheet about 3-10 m thick is exposed along the east side of a tributary of Cienega Creek (UTM 531395E, 3542796N to 531085E, 3542304N). In a small side canyon at UTM 531176E, 3542413N a buttress contact between the breccia and enclosing mudstone is well exposed.

Upper Pantano Formation

This unit includes strata lithologically similar to units Tpf and Tpc of the undivided Pantano Formation, but are interpreted to overlie the porphyritic andesite unit (unit Ta).

Tdu **Upper Pantano Formation, undivided (Oligocene to early Miocene).** Strata that are stratigraphically above the andesite of map unit Ta but have not been divided on the basis of lithologic criteria. Consists mostly of conglomerate and sandstone. Upper Pantano Formation conglomerates commonly contain sparse clasts of porphyritic andesite and other volcanic rocks resembling units Ta, Tap, or Tdt.

Tduf **Fine-grained siltstone and claystone, upper unit (Oligocene to early Miocene).** Siltstone, silty clay, and clay, with local gypsum beds up to several cm thick. Color of clay is variable, and includes pale yellow, pale green, tan, and brown. Locally includes sandstone and sparse pebbly conglomerate. Fine grained strata appear to be interbedded in upper conglomerate unit in the area east of Davidson Canyon. Along the railroad tracks adjacent to Cienega Creek west of Marsh Station Bridge, fine-grained sediment of the upper Pantano Formation grades west, apparently up section, into conglomerate.

Tduc **Coarse-grained sandstone and conglomerate, upper unit (Oligocene to early Miocene).** Massive to moderately well bedded, poorly sorted, pebble to boulder conglomerate. Locally includes sandstone and granule to pebbly sandstone. Clasts are mostly 3-30 cm and are locally as large as 2 m. Many smaller clasts are subangular, most others are subrounded. Colors are highly variable, and include tan, brown, and pale gray to greenish gray. Clasts compositions vary greatly over the area of exposure.

Volcanic Rocks interbedded in Pantano Formation

Tas **Andesitic volcaniclastic rocks (Oligocene to early Miocene)—**Massive to crudely bedded, volcanic lithic conglomerate, agglomerate, and/or breccia and coarse sandstone that is typically so massive and indurated that it is locally difficult to distinguish from lava flows of map unit Ta. Locally includes thin- to medium-bedded volcaniclastic sandstone and pebbly sandstone mixed with greenish mafic pyroclastic beds.

Tap **Crystal poor andesite (Oligocene).** Several small outcrops of medium gray, crystal-poor andesite(?) that overlies the porphyritic andesite or tuff unit. Observed adjacent to Cienega Creek, west of Marsh Station Bridge.

Tt **Tuff (Oligocene).** White to very light gray crystal –poor tuff, and associated tuffaceous sediment.

Ta **Porphyritic andesite lava flows (Oligocene)—**Porphyritic, crystal-rich, andesite lava flows. Contains conspicuous plagioclase phenocrysts up to 3 cm diameter in a medium to dark gray aphanitic matrix. Phenocrysts make up 20 to 40% of the rock. Locally near top of unit includes crystal poor to aphyric andesite lava flows (Vail Quadrangle).

Distinctive appearance of this rock has resulted in the informal name "turkey track porphyry" [e.g., Cooper, 1961]. Cooper [1961] recognized the regional character of this distinctive rock, and identified some petrographic features, including the composition of plagioclase ($An_{52\pm6}$), the general lack of zoning in plagioclase phenocrysts except oscillatory zoning, and the presence of small amounts of hypersthene and augite. (Cooper did not report petrographic information for andesite samples from the study area.) Although it has been proposed that this rock unit, present in many areas in southeastern Arizona, was derived from a single magma body, this has not been rigorously demonstrated. Two samples that were analyzed contained 55.5 and 52.5% SiO_2 [Cooper, 1961]. Mielke [1964] determined that the average K_2O and Na_2O content of 19 samples from widely scattered localities was 3.04% and 3.50%, respectively.

A sample of this unit, from near the railroad bridge over Cienega Creek 2 km west of the map area, yielded a K-Ar date of 24.9 ± 5.2 Ma (2σ uncertainty [95% confidence interval]), and a sample from the northeastern Rincon Mountains (Mineta Ridge) yielded an age of 26.9 ± 4.8 Ma (2σ uncertainty [95% confidence interval]; Shafiqullah et al., 1978). A sample from the Del Bac Hills, south of the Tucson Mountains and west of the map area, yielded dates of 26.3 ± 1.6 Ma (plagioclase), 27.3 ± 1.6 Ma (HF-leached plagioclase(?)) and 26.9 ± 1.6 Ma (groundmass without magnetic fraction) (Percious, 1968; 2σ uncertainty [95% confidence interval] for all). The age of this rock is estimated to be 26 to 27 Ma.

Lower Pantano Formation

This unit includes strata lithologically similar to units Tpf and Tpc of the undivided Pantano Formation, but are interpreted to underlie the porphyritic andesite unit (unit Ta).

Tdl **Lower Pantano Formation (Oligocene to early Miocene).** Strata that are stratigraphically below the andesite of map unit Ta but have not been divided on the basis of lithologic criteria.

Tdlf **Fine-grained siltstone and claystone, lower unit (Oligocene to early Miocene)—** Siltstone, silty clay, and clay. One poorly exposed outcrop area on the east side of Davidson Canyon near the southern edge of the map area.

Tertiary igneous rocks

Tr **Rhyolitic tuff (Oligocene)**—Pale gray to whitish gray, crystal-rich, densely welded, rhyolitic tuff beneath Pantano Formation, with phenocrysts of quartz, plagioclase, sanidine, and biotite.

This tuff was dated at 33.01 ± 0.38 Ma (weighted mean of six single-crystal $^{40}Ar/^{39}Ar$ sanidine dates from unpublished report by Lisa Peters, New Mexico Bureau of Mines and Mineral Resources [1999], sample 5-6-98-1; 2σ uncertainty). Previously determined dates are as follows: 33.6 ± 5.4 Ma (K-Ar biotite), and 37.6 ± 2.2 Ma (K-Ar sanidine; both by Damon and Bikerman, 1964, given as recalculated by Reynolds et al., 1986), and 34.4 ± 1.6 Ma (K-Ar biotite; Dickinson and Shafiqullah, 1989; 2σ uncertainty [95% confidence interval] given for all dates).

Tf **Felsite dike (Tertiary?)**—About 200 m north of Pump Canyon near the southern edge of the Narrow 7 ½' Quadrangle a felsic dike contains 2-3%, 1-3 mm quartz.

Mesozoic map units

Bisbee Group

The late Jurassic to middle Cretaceous Bisbee Group of southeastern Arizona and adjacent parts of New Mexico, Sonora, and Chihuahua, was deposited in a structurally complex rift trough produced by late Jurassic rifting. This rifting occurred in an area that had previously been subject to Jurassic, subduction-related magmatism. The basal Glance Conglomerate member of the Bisbee Group was deposited in basins flanking uplifted fault blocks within the rift trough, and is characterized by large changes in thickness and clast composition over short distances. The overlying finer grained strata of the Bisbee Group were deposited as the rift topography was erosionally degraded and buried [Bilodeau et al., 1987; Dickinson et al., 1987, 1989].

The basal unit of the Bisbee Group, the Glance Conglomerate (map unit KJg), varies greatly in thickness and composition in the surrounding region. In the central Empire Mountains (south of the map area), where it overlies Paleozoic units, the Glance Conglomerate consists of coarse-grained, massive conglomeratic rocks that thin rapidly to the south. In the hills north of the north end of the Empire Mountains (including outcrops in the southeast corner of the map area), Glance Conglomerate directly overlies

Proterozoic basement, and the Bisbee Group consists of a relatively thin sequence of arkosic sandstone and monolithic granitoid-clast conglomerate. Locally, some of this conglomerate includes lenses with abundant carbonate clasts.

Kb **Sandstone, mudstone, and associated rocks (Cretaceous)**—Thin- to thick-bedded, fine- to coarse-grained sandstone and silty sandstone. Commonly includes sparse pebbly sandstone beds and olive gray, commonly pyrite-bearing siltstone and mudstone. Examination with hand lens suggests that arkosic and quartzofeldspathic compositions are most common. Pebbly sandstone beds contain abundant black and white, well-rounded to rounded chert clasts. Thin- to medium-bedded limestone beds occur in some areas. Gypsum beds several to, rarely, several tens of cm thick are locally associated with shaley sediments that also contain silty carbonate thin beds. Thin limestone beds tend to be laminated, and the medium-bedded limestone (rarely thick-bedded) are commonly mollusk shell, skeletal wackstone with dark micritic, fetid matrix. Mudcracks are present locally, as are redbeds. Color is typically greenish gray with less common brownish or orangish gray and medium brown. Cleavage is locally developed, in some areas strongly so, in fine-grained rocks. Magnetite laminations locally form low angle cross beds with truncations that reveal stratigraphic top direction. Sandstone is dominant at lower stratigraphic levels, with increasingly abundant siltstone at higher stratigraphic levels.

Locally includes massive volcanic lithic conglomerate with 2-20 cm subrounded clasts of greenish gray, crystal poor, quartz-absent volcanic rocks and sparse fragments of flattened pumice(?) (outcrops located along railroad tracks next to Cienega Creek just west of eastern edge of map area).

KJg **Glance conglomerate, undivided (lower Cretaceous to upper Jurassic)**—Conglomerate, coarse-grained arkose, and rare limestone are present locally at the base of the Bisbee Group. Generally consists of clast-supported, rounded to sub-rounded cobble-boulder units containing mostly granodiorite clasts.

Gardner Canyon Formation (Jurassic – Triassic)—A heterolithic assemblage of dark red mudstone or slate, volcaniclastic sandstone, and conglomerate, with sparse volcanic flows. Estimated at up to 350 meters thick by Finnell (1971).

JTRgm **Mudstone, Gardner Canyon Formation (Jurassic – Triassic)**—Dark red mudstone or slate, typically strongly cleaved.

JTRlv **Limestone and volcaniclastic rocks (Jurassic – Triassic)—**Strongly cleaved silvery gray mudstone with very thin interbedded fine-grained sandstone, volcaniclastic conglomerate, and sparse lenses of limestone 2-5 cm thick and 10-30 cm long parallel to the foliation in the outcrop. Some limestone may flattened diagenetic/metamorphic nodules.

JTRgs **Sandstone (Jurassic – Triassic)**— Sandstone, volcaniclastic conglomerate, and mudsonte. A single exposure in the core of a syncline in strongly deformed package of rock adjacent to faults against Tertiary and Paleozoic rocks..

Paleozoic map units

Pl **Carbonate rocks (Upper Paleozoic?)**—Massive gray dolostone and calcareous dolostone forms a small outcrop area adjacent to strongly cleaved mudstone and fine-grained sandstone of .

Scherrer Formation (Permian)

Ps **Quartizte** -- Medium to fine grained shattered quartzite and laminated red-brown fine-grained quartz arenite. Massive to weakly laminated, pale gray to whitish gray on fresh surfaces, pale orangish brown weathering quartzite forms hill, and red-brown sandstone is exposed in wash north of hill. Contact with lower Epitaph Formation to north is faulted, and southern end of outcrop is covered. Probably equivalent to lower Scherrer Formation in adjacent quads to east and south.

Marker bed. Medium to light gray dolostone lithologically similar to that in unit Psm, interbedded in quartzite. Marker is about 3 m thick.

Psm **Dolostone**-- Medium-bedded, medium to light gray dolostone packstone to grainstone and very fine grained crystalline carbonate, contains some 5 to 25 cm long chert nodules and stringers. Plane lamination and small-scale low-angle cross laminations visible in some places. Single isolated outcrop south of quartzite hill (UTM 532382E, 3544900N).

Epitaph Formation (Permian)—Medium to dark gray massive carbonate with numerous, thin

Pel **Lower Dolostone**—Medium to dark gray, medium- to thick-bedded dolostone. Dolomite is apparently micrite, packstone and fine-grained grainstone. Fossils are rare. Plane lamination and small-scale ripple cross-bedding are locally visible in the dolostone. Lenses of fine-grained quartzose sandstone are present. Because of structural disruption, it is unclear how many of these sandstone beds are present in the section. Thin white carbonate veinlets filling fractures are ubiquitous.

PPe **Earp Formation (Pennsylvanian to Permian)**—Highly variable assemblage of alternating sandstone, dolostone, limestone, mudstone, and sparse conglomerate. Sandstone is very fine-grained to fine-grained, quartz-rich, and is calcareous or non-calcareous. Color is variable including pale greenish and tannish buff, grayish tan, and pale to medium reddish brown. Also includes thin- to medium-bedded limestone with partings along thin beds of silty carbonate and very fine grained sandstone. Some limestone contains sparse chert stringers 1-3 m thick. Several zones of terra rosa siltstone suggest multiple episodes of sub aerial weathering. Conglomerate includes several 1-3 m thick beds of chert or chert-carbonate pebble-cobble conglomerate, which occur in the lower middle(?) part of the formation (mapped as marker bed). Contact with the overlying lower dolostone of the Epitaph Formation is placed at the base of a prominent interval of medium-bedded, dark gray dolostone. The contact with the underlying Horquilla formation is difficult to define precisely, and has been placed at the base of the lowest sandstone or shale bed that overlies massive to thick limestone beds that contain less than 50% interbedded sandstone.

Chert-pebble conglomerate marker bed. Chert fragments up to 10 cm in diameter are present. Beds are 1-3 m thick, and consist of chert and limestone or dolostone pebbles to cobbles in a matrix of sandy limestone or calcareous sandstone. Chert clasts are angular to subround reddish-gray to brown chert granules to cobbles up to 5 cm diameter. Carbonate clasts are subrounded light gray limestone or dolostone. Finer-grained parts of conglomerate beds display planar bedding or low-angle cross bedding.

Ph **Horquilla Limestone (Pennsylvanian)**—Medium gray, massive to thick-bedded limestone with occasional cherty beds, silty carbonate beds, and sandstone beds. Some light or dark gray carbonate beds are present. Where primary carbonate textures are visible on weathered surfaces, rocks appears to be mostly grainstone or packstone. Some chert-rich beds are present, and sparse dark gray chert nodules and stringers are present throughout the unit. Some zones of brecciated carbonate with hematitic matrix are present. A few beds of reddish brown siltstone and tan, fine-grained quartzose sandstone are also present. One sandstone bed was mapped as a marker horizon (UTM 532157E, 3545759N). The interbedded units with siliciclastic components tend to be non-resistant, and probably form many of the swales between thick carbonate beds.

The contact with the Escabrosa Limestone is poorly exposed. It is marked by a thin discontinuous reddish, mud-matrix fragmental deposit interpreted to represent a weathering horizon. This deposite is mapped as unit Mek where thick enough to show. Where this unit is absent the contact is very difficult to locate precisely, and is generally placed where bedding partings become more visible and interbedded siliciclastic-bearing units become apparent.

Marker bed. Tan fine-grained quartz arenite, about 4 m thick.

Me$_k$ **Karst deposits (Mississippian or Pennsylvanian(?))**—Karst deposits. Where exposed about 1 km east of Colossal cave, the zone is about 50 cm thick, and consists of carbonate clasts surrounded by a reddish brown siliceous (argillaceous?) matrix, with a 10 to 20 cm thick central zone of reddish brown siltstone [Spencer et al., 2002]. Also includes reddish-brown mudstone, clay-rich quartz sandstone, and sandy chert pebble conglomerate.

Me **Escabrosa Limestone (Mississippian)**—Pale gray to medium gray, very finely crystalline limestone with sparse, irregular, siliceous nodules 1-10 cm thick and up to 1 m long along bedding. Sparse, solitary horn coral fossils are present in the upper part. Limestone is generally massive. Where primary depositional textures are visible, rock is grainstone, commonly containing abundant crinoid columnals; medium- to large-scale (0.5-1.5 m thick) cross-sets are sometimes visible. The Escabrosa Limestone is massive and homogeneous compared to the Horquilla Limestone.

Dm **Martin Formation (Devonian)**—Pale gray to medium gray, micritic to sandy dolostone and limestone, locally with sparse chert nodules and stringers. Typically dolomitic, with rare clean quartzite beds up to several tens of cm thick. Uniform thin to medium planar bedding is characteristic. The unit is poorly exposed in this area, and definition of a clear contact with the Escabrosa Limestone and Abrigo Shale is not possible. Dolomitic beds with variable amounts of quartz sand are interbedded with thick to massive limestone at the contact with Escabrosa Limestone in the northeastern part of the map area (UTM 535059E, 3547526N) in an interval of about 10 m of strata separating clear Escabrosa and Martin formations. Contact with the Abrigo Shale is more poorly exposed and tenuous, and has been places where quartz sand becomes a ubiquitous component of strata down section.

Ꞓa **Abrigo Shale (Cambrian)—**Carbonate, siltstone, and sandstone of the Abrigo Shale. Upper part consists of tan to brown, sandy and silty, recrystallized limestone, and light to dark brown weathering, laminated carbonate with very fine grained sand (sandy carbonate). Lower part of unit consists of calcareous and non-calcareous siltstone and fine grained sandstone with sparse trace fossils. Locally includes medium and coarse quartz sand grains in sandy carbonate.

In a good exposure in the adjacent Rincon Peak Quadrangle [Spencer et al., 2002] the upper contact is sharp and is placed above a sandy carbonate unit consisting of numerous 3 to 30 cm thick, protruding quartzite and calcareous quartzite layers and gray, recess forming limestone. The overlying Martin Formation is a 6-8 meter cliff composed of massive, orangish brown dolostone.

Ꞓq **Bolsa Quartzite (Cambrian)--**Fine- to coarse-grained, thin- to thick-bedded, resistant quartzite (>95% quartz) and feldspathic quartzite. Includes coarse, granule sandstone with local pebbles, and local thin beds (up to 1 cm thick) containing abundant quartz granules and small pebbles 2-7 mm diameter. Dark laminations rich in magnetite reveal cross bedding and are characteristic regionally of Cambrian Bolsa Quartzite in areas where Proterozoic diabase was exposed during initial Cambrian sedimentation. Commonly blocky weathering.

Hill top and east side of hill about 1.2 km southwest of Colossal Cave (UTM 534000E, 3546300N) consists of pure quartzite containing very little opaque mineral, which is generally too massive to see bedding. This rock may be Proterozoic Dripping Spring Quartzite instead of Cambrian Bolsa Quartzite. This interpretation is not made on the map, however, because Dripping Spring Quartzite commonly contains significant K-feldspar, which was not observed.

Proterozoic map units

Apache Group and associated Sierra Ancha diabase

Yd **Sierra Ancha diabase (Middle Proterozoic)**—Dark greenish gray diabase with acicular plagioclase laths up to 4 mm long and dark clinopyroxene(?). Typically non-resistant to weathering, and form characteristic dark greenish gray to brown soil.

Yp **Pioneer Formation, Apache Group (Middle Proterozoic)—**Variably silty quartzose sandstone and very fine grained silty sandstone and sandy siltstone. Unlike poorly to moderately well sorted sandstone in the Cambrian Bolsa Quartzite, Pioneer Formation sandstone is typically well sorted. Colors include light to dark brown, medium gray, and reddish brown. Reduction spots, which are common elsewhere in the Pioneer Formation [Wrucke, 1989], were not seen. The base of Pioneer Formation is a 10 to 100 cm thick zone that contains abundant subangular fragments of vein quartz up to 10 cm diameter in a matrix of coarse to granule arkose. This basal conglomerate, known as the Scanlon Conglomerate member, overlies weathered and discolored granitoids of map unit YXg. On Pistol Hill the bottom 1-5 meters of the Pioneer Formation, above the basal conglomerate, contains sparse to abundant 1-10 cm subangular fragments of vein quartz. Overlying sandstone is medium to fine grained quartzite and silty quartzite. Near base sandstone is medium to coarse grained orthoquartzite that contains 1-2% magnetite; some magnetite-rich laminations are present.

The top of the unit in this map area is a poorly exposed intrusive contact with diabase (Unit Yd). Spotted hornfels textures due to contact metamorphism are present in some silty rocks. These strata are correlated with the formal unit defined by Ransome [1919], based on lithology and stratigraphic position, following Drewes [1977].

Early to Middle Proterozoic crystalline rock units

Rincon Valley Granodiorite (Drewes [1977]; formally named after earlier designation as granodiorite of Rincon Valley by Drewes [1974]) is the name applied to an extensive granitoid unit exposed in and around the Rincon Mountains. Eight radiometric age determinations listed by Reynolds et al. [1986] for the Rincon Valley Granodiorite range from 1340 to 1570 Ma, with 5 of 8 dates ranging from 1390 to 1460 Ma (dates from Marvin et al. [1973] and Marvin and Cole [1978]). The eight dates were from four samples: Two from northwestern Saguaro East National Park (Marvin and Cole [1978]; locations plotted by Drewes [1977]), one from Rincon Valley about 2 km northeast of Colossal Cave [Marvin et al., 1973], and one from the Happy Valley area on the east side of the Rincon Mountains [Marvin et al., 1973]. The two dates that are older than 1460 Ma have large uncertainties (1550 ± 60 Ma, K-Ar biotite; 1570 ± 100 Ma, K-Ar hornblende). Furthermore, these uncertainties are at the 1σ level, which means that the 95% confidence interval (2σ) is twice as large (Robert Fleck, USGS, written communication, 2001). Given the uncertainty in the two older dates, and the clustering of the other ages around 1400 Ma, it seems likely that the Rincon Valley Granodiorite cooled through the argon closure temperature for biotite and muscovite at about 1400 Ma.

Mapping done as part of this report identified two granitoids in the area mapped as Rincon Valley Granodiorite by Drewes [1977]: One is a porphyritic biotite granite, and the other is a medium grained, non-porphyritic granodiorite(?). The granodiorite resembles other 1.7 Ga rocks in southeastern Arizona, and we consider it likely that the granodiorite is Early rather than Middle Proterozoic. The porphyritic biotite granite is lithologically similar to 1.4 granites in southeastern Arizona, and we consider it likely that this granite is Middle Proterozoic. Furthermore, intrusion of the Middle(?) Proterozoic granite may be at least partly responsible for the Middle Proterozoic radiometric ages derived from the granodiorite. These two granitoids were only differentiated over a small area in the northeastern part of the map area.

YXg **Porphyritic granite (Middle Proterozoic)—**medium- to coarse-grained, slightly porphyritic biotite granite. Non-resistant to weathering, forms extensive pediment in the northeastern corner of the map area. Near the fault that juxtaposes this granite with unit Xgd (UTM 533685E, 3549039N), consists of 15-20% K-feldspar up to 1.5 cm in diameter, 25-30% quartz 2-6 mm in diameter, 50-60% plagioclase 2-5 mm in diameter, and 5% biotite in 2-3 mm diameter flakes. Biotite is variably altered to chlorite. This granite is distinctly less iron stained than granodiorite (unit Xgd) southwest of the fault. Boundary with unit Xgd was not mapped along the boundary between this map area and Spencer et al. [2002] map of the adjacent Rincon Peak quadrangle.

Xgd **Granodiorite (Early to Middle Proterozoic)—**Equigranular, medium- to fine-grained granite or granodiorite with biotite, hornblende(?), and secondary chlorite. Probably equivalent to Rincon Valley Granodiorite of Drewes [1977] but suspected to be Early Proterozoic based on lithologic dissimilarity to 1.4 Ga granites in southeastern Arizona (see above). This rock is probably related to Early Proterozoic granodiorite in the adjacent quadrangles to the south and east [Ferguson et al., 2001; Spencer et al., 2002].

Xp **Pinal Schist (Middle Proterozoic)—**Pale-gray to medium-gray schist and psammitic schist that is sufficiently metamorphosed that pelitic rocks have significant phyllosilicate development and cleavage parallel to preferred orientation of phyllosilicates. Phyllosilicates, locally visible in hand sample without the aid of a hand lens, impart a silvery sheen to the rock. Also, quartz veins and stringers are locally abundant, especially in pelitic rocks.

REFERENCES CITED

Anderson, S.R., 1988, Potential for aquifer compaction, land subsidence, and earth fissures in the Tucson basin, Pima County, Arizona: U.S. Geological Survey Hydrologic Investigations Atlas HA-713, 3 sheets, scale 1:250,000.

Anderson, S.R., 1989, Potential for aquifer compaction, land subsidence, and earth fissures in Avra Valley, Pima and Pinal Counties, Arizona: U.S. Geological Survey Hydrologic Investigations Atlas HA-718, 3 sheets, scale 1:250,000.

Archibald, L.E., 1987, Stratigraphy and sedimentology of the Bisbee Group in the Whetstone Mountains, southeastern Arizona, *in* Dickinson, W.R., and Klute, M.A., eds., Mesozoic rocks of southern Arizona and adjacent areas: Arizona Geological Society Digest, v. 18, p. 273-282.

Arizona Geological Survey, 1988, Earth fissures discovered near CAP canals: Arizona Geology, v. 18, n. 4, p. 10.

Balcer, R. A., 1984, Stratigraphy and Depositional History of the Pantano Formation (Oligocene-Early Miocene), Pima County, Arizona: Tucson, University of Arizona, 107 pages.

Banks, N.G., 1980, Geology of a zone of metamorphic core complexes in southeastern Arizona, *in* Crittenden, M.D., Jr., Coney, P.J., and Davis, G.H., eds., Cordilleran metamorphic core complexes: Geological Society of America Memoir 153, p. 177-215.

Betancourt, J.L., 1990, Tucson's Santa Cruz River and the arroyo legacy: unpublished Ph.D. dissertation, University of Arizona, 239 p.

Bilodeau, W.L., 1979, Early Cretaceous tectonics and deposition of the Glance Conglomerate, southeastern Arizona: California, Stanford University, Ph.D. dissertation, 145 p.

Bilodeau, W.L., Kluth, C.F., and Vedder, L.K., 1987, Regional stratigraphic, sedimentologic and tectonic relationships of the Glance Conglomerate in southeastern Arizona, *in* Dickinson, W.R., and Klute, M.A., eds., Mesozoic rocks of southern Arizona and adjacent areas: Arizona Geological Society Digest, v. 18, p. 229-256.

Bilodeau, W.L., Kluth, C.F., and Vedder, L.K., 1987, Regional stratigraphic, sedimentologic and tectonic relationships of the Glance Conglomerate in southeastern Arizona, *in* Dickinson, W.R., and Klute, M.A., eds., Mesozoic rocks of southern Arizona and adjacent areas: Arizona Geological Society Digest, v. 18, p. 229-256.

Brennan, D.J., 1957, Geological reconnaissance of Cienega Gap, Pima County, Arizona: Tucson, University of Arizona, Ph.D. dissertation, 53 p.

Brennan, D.J., 1962, Tertiary sedimentary rocks and structures of the Cienega Gap area, Pima County, Arizona, *in* Heindl, L.A., ed., Cenozoic geology of Arizona - a symposium: Arizona Geological Society Digest, v. 5, p. 45-57.

Bull, W.B., 1991, Geomorphic Response to Climatic Change, New York: Oxford University Press, 326 p.

Bull, W.B., and Pearthree, P.A., 1988, Frequency and size of Quaternary surface ruptures on the Pitaycachi fault, northeastern Sonora, Mexico: Bull. Seis. Soc. Amer., v. 78, p. 956-978.

Cooper, J.R., 1961, Turkey-track porphyry—a possible guide for correlation of Miocene rocks in southeastern Arizona: Arizona Geological Society Digest, v. 4, p. 17-33.

Creasey, S.C., 1967, Geologic map of the Benson quadrangle, Cochise and Pima Counties, Arizona [McGrew Spring, Apache Peak, Benson, and Mescal 7.5 min]: U.S. Geological Survey Miscellaneous Geologic Investigations Map I-470, 11 p., 1 sheet, scale 1:48,000.

Damon, P.E., and Bikerman, M., 1964, Potassium-argon dating of post-Laramide plutonic and volcanic rocks within the Basin and Range province of southeastern Arizona and adjacent areas: Arizona Geological Society Digest, v. 7, p. 63-78.

Damon, P.E., Erickson, R.C., and Livingston, D. E., 1963, K-Ar dating of Basin and Range uplift, Catalina Mountains, Arizona: National Academy of Sciences/National Research Council Publication 1075, Nuclear Science Series, report 38, Woods Hole Conference on Nuclear Geophysics, p. 113-121.

Davis, G.A., and G.S. Lister, 1988, Detachment faulting in continental extension; Perspectives from the southwestern U.S. Cordillera, *in* Clark, S.P., Jr., Burchfiel, B.C., and Suppe, J., eds., Processes in continental lithosphere deformation: Geological Society of America Special Paper 218, p. 133-160.

Davis, G.H., 1975, Gravity-induced folding off a gneiss dome complex, Rincon Mountains, Arizona: Geological Society of America Bulletin, v. 86, no. 7, p. 979-990.

Davis, G.H., 1980, Structural characteristics of metamorphic core complexes, southern Arizona, *in* Crittenden, M.D., Jr., Coney, P.J., and Davis, G.H., eds., Cordilleran metamorphic core complexes: Geological Society of America Memoir 153, p. 35-77.

Demsey, K.A., and Pearthree, P.A., 1994, Surficial and environmental geology of the Sierra Vista area, Cochise County, Arizona: Arizona Geological Survey Open-File Report 94-6, 14 p., scale 1:24,000.

Demsey, K.A., House, P.K., and Pearthree, P.A., 1993, Detailed surficial geologic map of the southern piedmont of the Tortolita Mountains, Pima County, southern Arizona: Arizona Geological Survey Open-File Report 93-14, 8 p. scale 1:24,000.

Dickinson, W.R., 1991, Tectonic setting of faulted Tertiary strata associated with the Catalina core complex in southern Arizona: Geological Society of America Special Paper 264, 106 p., 1 sheet, scale 1:125,000.

Dickinson, W.R., and Shafiqullah, Muhammad, 1989, K-Ar and F-T ages for syntectonic mid-Tertiary volcanosedimentary sequences associated with the Catalina core complex and San Pedro trough in southern Arizona: Isochron/West, n. 52, p. 15-27.

Dickinson, W.R., Fiorillo, A.R., Hall, D.L., Monreal, R., Potochnik, A.R., and Swift, P.N., 1989, Cretaceous strata of southern Arizona, *in* Jenny, J.P., and Reynolds, S.J., eds., Geologic evolution of Arizona: Arizona Geological Society Digest 17, p. 397-434.

Dickinson, W.R., Klute, M.A., and Bilideau, W.L., 1987, Tectonic setting and sedimentologic features of Upper Mesozoic strata in southeastern Arizona, *in* Davis, G.H., and VandenDolder, E.M., eds., Geologic diversity of Arizona and its margins: Excursions to choice areas: Arizona Geological Survey Special Paper 5, p. 266-279.

Dobyns, H.R., 1981, From fire to flood, Historic human destruction of Sonoran desert riverine oases, 222 p., Ballena Press, Socorro, NM.

Drewes, H.D., 1974, Geologic map and sections of the Happy Valley quadrangle, Cochise County, Arizona: U.S. Geological Survey Miscellaneous Investigations Series Map I-832, 1 sheet, scale 1:48,000.

Drewes, H.D., 1977, Geologic Map and Sections of the Rincon Valley Quadrangle, Pima County, Arizona: U.S. Geological Survey Miscellaneous Investigations Series Map I-977, 1 sheet, scale 1:48000.

DuBois, S.M., Smith, A.W., Nye, N.K., and Nowak, T.A., 1982, Arizona Earthquakes, 1776-1980: Arizona Bureau of Geology and Mineral Technology Bulletin 193, 456 p., scale 1:1,000,000.

Finnell, T.L., 1970, Formations of the Bisbee Group, Empire Mountains quadrangle, Pima County, Arizona, in Changes in stratigraphic nomenclature by the U.S. Geological Survey, 1968: U.S. Geological Survey Bulletin 1294-A, p. A28-A35.

Finnell, T.L., 1971, Preliminary geologic map of the Empire Mountains quadrangle, Pima County, Arizona: U.S. Geological Survey Open-File Report 71-0106, 2 sheets, scale 1:48,000.

Force, E.R., 1997, Geology and mineral resources of the Santa Catalina Mountains, southeastern Arizona: Tucson, Arizona, Center for Mineral Resources, Monographs in Mineral Resource Science, n. 1, 134 p.

Fournier, R.O., 1985, Silica minerals as indicators of conditions during gold deposition, *in* Tooker, E.W., Ed., Geologic characteristics of sediment- and volcanic-hosted disseminated gold deposits—search for an occurrence model: Washington, D.C., U. S. Geological Survey Bulletin, 1646, p. 15-26.

Galloway, Devin, Jones, David R., and Ingerbritsen, S.E., 1999, Land subsidence in the United States: US Geological Survey Circular 1182, 177 p.

Gile, L.H., Hawley, J.W., and Grossman, R.B., 1981, Soils and geomorphology in the basin and range area of southern New Mexico -- guidebook to the Desert Project: New Mexico Bureau of Mines and Mineral Resources Memoir 39, 222 p.

Hansen, W.R., 1991, Suggestions to authors of the reports of the United States Geological Survey: U.S. Government Printing Office, 7th edition, 289 p.

Hatch, M.A., 1991, Global positioning system measurement of subsidence in the Tucson Basin, Pima County, Arizona: Tucson, University of Arizona, M.S. thesis, 87 p.

Jackson, G.W., 1989, Surficial geologic maps of the northeastern, southeastern, and southwestern portions of the Tucson metropolitan area: Arizona Geological Survey Open-File Report 89-2, 6 p., 7 sheets, scale 1:24,000.

Jackson, G.W., 1990, Quaternary geologic map of the Corona de Tucson 7.5' quadrangle, Arizona: Arizona Geological Survey Open-File Report 90-3, 6 p., scale 1:24,000.

Johnson, R.A., and Loy, K.L., 1992, Seismic reflection evidence of seismogenic low-angle faulting in southeastern Arizona: Geology, v. 20, n. 7, p. 597-600.

Katzer, Keith, and Schuster, J.H., 1984, The Quaternary geology of the northern Tucson basin, Arizona and its archaeological implications: Tucson, University of Arizona Dept. of Geosciences, M.S. prepublication manuscript.

Keith, S. B., Reynolds, S. J., Damon, P. E., Shafiqullah, M., Livingston, D. E., and Pushkar, P. D., 1980, Evidence for multiple intrusion and deformation within the Santa Catalina-Rincon-Tortolita crystalline complex, southeastern Arizona, *in* Crittenden, M. D., and others, G. H., eds., Cordilleran metamorphic core complexes: Geological Society of America Memoir 153, p. 217-267.

Keith, S.B., Gest, D.E., DeWitt, Ed, Woode Toll, Netta, and Everson, B.A., 1983, Metallic mineral districts and production in Arizona: Arizona Bureau of Geology and Mineral Technology Bulletin 194, 58 p., 1 sheet, scale 1:1,000,000.

Klawon, J.E., Dickinson, W.R., and Pearthree, P.A., 1999, Surficial geology and geologic hazards of the northern Tucson basin, Tucson North and Sabino Canyon 7 ½' quadrangles: Arizona Geological Survey Open-File Report 99-21, 21 p. 1 sheet, scale 1:24,000.

Klute, M.A., 1991, Sedimentology, sandstone petrofacies, and tectonic setting of the late Mesozoic Bisbee basin, southeastern Arizona: Tucson, University of Arizona Ph.D. dissertation, 268 p.

Layton, D.W., 1957, Stratigraphy and structure of the southwestern foothills of the Rincon Mountains, Pima County, Arizona: Tucson, University of Arizona, M.S. thesis, 87 p.

Liebler, Gail S., 1988, Geology and gold mineralization at the Picacho Mine, Imperial County, California, *in* Schafer, Robert W., Cooper, James J., and Vikre, Peter G., Editors, Bulk Mineable Precious Metal Deposits of the Western United States, Symposium Proceedings: Reno, NV, The Geological Society of Nevada, p. 453-472.

Lister, G.S., and Davis, G.A., 1989, The origin of metamorphic core complexes and detachment faults formed during Tertiary continental extension in the northern Colorado River region, U.S.A.: Journal of Structural Geology, v. 11, p. 65-94.

Machette, M.N., 1985, Calcic soils of the southwestern United States: in Weide, D.L., ed., Soils and Quaternary Geology of the Southwestern United States: Geological Society of America Special Paper 203, p. 1-21.

Marvin, R.F., and Cole, J.C., 1978, Radiometric ages; compilation A, U.S. Geological Survey: Isochron/West, n. 22, p. 3-14.

Marvin, R.F., Stern, T.W., Creasey, S.C., and Mehnert, M.H., 1973, Radiometric ages of igneous rocks from Pima, Santa Cruz, and Cochise Counties, southeastern Arizona: U.S. Geological Survey Bulletin 1379, 27 p.

McKee, E.D., and Weir, G.W., 1953, Terminology for stratification and cross-stratification in sedimentary rocks: Geological Society of America Bulletin, v. 64, p. 381-390.

McKittrick, M.A., 1988, Surficial geologic maps of the Tucson metropolitan area: Arizona Geological Survey Open-File Report 88-18, 7 p., 12 sheets, scale 1:24,000.

Menges, C.M., and McFadden, L.D., 1981, Evidence for a latest Miocene to Pliocene transition from Basin-Range tectonic to post-tectonic landscape evolution in southeastern Arizona: Arizona Geological Society Digest 13, p. 151-160.

Menges, C.M., and Pearthree, P.A., 1989, Late Cenozoic tectonism and landscape evolution in Arizona, in Jenney, J., and Reynolds, S.J., eds., Geologic Evolution of Arizona: Arizona Geological Society Digest 17, p. 649-680.

Metz, R.A., 1963, The petrography of the Pantano Beds in the Cienega Gap area, Pima County, Arizona: Tucson, University of Arizona, M.S. thesis, 66 p.

Mielke, J.E., 1964, Trace element investigation of the 'Turkey Track' porphyry, southeastern Arizona: Arizona Geological Society Digest, v. 7, p. 87-96.

Myrick, David F., 1975, Railroads of Arizona Vol. 1; the southern roads, Berkeley, California, Howell-North Books.

Parker, J.T.C., 1995, Channel change on the Santa Cruz River, Pima County, Arizona: U.S. Geological Survey Water-Supply Paper 2429, 58 p.

Pearthree, P.A., 1986, Late Quaternary faulting and seismic hazard in southeastern Arizona: Arizona Geological Survey Open-File Report 86-8, 22 p.

Pearthree, P.A., 1998, Quaternary fault data and map for Arizona: Arizona Geological Survey Open-File Report 98-24, 122 p., map scale 1:750,000.

Pearthree, M.S., and Baker, V.R., 1987, Channel change along the Rillito Creek system of southeastern Arizona, 1941 through 1983; Implications for flood-plain management: Arizona Geological Survey Special Paper 6, 58 p., scale 1:24,000.

Pearthree, P.A., and Biggs, T.H., 1999, Surficial geology and geologic hazards of the Tucson Mountains, Pima County, Arizona: Arizona Geological Survey Open-File Report 99-22, 12 p., 2 sheets, scale 1:24,000.

Pearthree, P.A., and Calvo, S.S., 1987, The Santa Rita fault zone: Evidence for large magnitude earthquakes with very long recurrence intervals, Basin and Range province of southeastern Arizona: Bull. Seis. Soc. Amer., v. 77, p. 97-116.

Pearthree, P.A., and Youberg, Ann, 2000, Surficial geologic maps and geologic hazards of the Green Valley – Sahuarita area, Pima County, Arizona: Arizona Geological Survey Open-File Report 00-13, 21 p., 2 sheets, scale 1:24,000.

Pearthree, P.A., Demsey, K.A., Onken, Jill, Vincent, K.R., and House, P.K., 1992, Geomorphic assessment of flood-prone areas on the southern piedmont of the Tortolita Mountains, Pima County, Arizona: Arizona Geological Survey Open-File Report 91-11, 31 p., 4 sheets, scale 1:12,000 and 1:24,000.

Peizhen, Z., Molnar, P., and Downs, W.R., 2000, Increased sedimentation rates and grain sizes 2-4 Myr ago due to the influence of climate change on erosion rates: Nature, v. 410, p. 891-897.

Percious, J.K., 1968, Geology and geochronology of the Del Bac Hills, Pima County, Arizona, *in* Titley, S.R., ed., Southern Arizona Guidebook III: Arizona Geological Society, p. 199-207.

Percival, T. J., Bagby, W. C., and Radtke, A. S., 1988, Physical and chemical features of precious metal deposits hosted by sedimentary rock sin the western United States, *in* Schafer, R.W., Cooper, J.J., and Vikre, P. G., Eds., Bulk Mineable Precious Metal Deposits of the Western United States, Symposium Proceedings: Reno, The Geological Society of Nevada, p. 11-33.

Platt, W.S., 1963, land-surface subsidence in the Tucson area: University of Arizona unpublished Masters Thesis, Department of Geology, 38 p.

Pope, G.L., Rigas, P.D., and Smith, C.F., 1998, Statistical summaries of streamflow data and characteristics of drainage basins for selected streamflow-gaging stations in Arizona through Water Year 1996: U.S. Geological Survey Water-Resources Investigations Report 98-4225, 907 p.

Ransome, F.L., 1919, The copper deposits of Ray and Miami: U.S. Geological Survey Professional Paper 115, 192 p., map-scale 1:125,000.

Reynolds, S.J., Florence, F. P., Welty, J. W., Roddy, M. S., Currier, D. A., Anderson, A. V., and Keith, S. B., 1986, Compilation of radiometric age determinations in Arizona: Tucson, Arizona Bureau of Geology and Mineral Technology Bulletin 197, 258 p.

Schumann, H.H., 1992, Land subsidence and earth-fissure hazards near Luke Air Force Base, Arizona, *in* U.S. Geological Survey Subsidence Interest Group conference, Edwards Air Force Base, Antelope Valley, California, November 18-19, 1992 - Abstracts and Summary: US Geological Survey Open-File Report 94-532, p. 18-21.Sellers, W.D., and Hill, R.H., 1974, Arizona Climate, 1931-1972: Tucson, University of Arizona Press, 616 p.

Scott, R. W., 1987, The bivalve, Musculiopsis MacNeill, in Lower Cretaceous non-marine strata, Rocky Mountains: Contributions to Geology, University of Wyoming, v. 25, p. 29-33.

Sellers, W.D., and Hill, R.H., 1974, Arizona Climate, 1931-1972: Tucson, University of Arizona Press, 616 p.

Shafiqullah, M., Damon, P. E., Lynch, D. J., Kuck, P. H., and Rehrig, W. A., 1978, Mid-Tertiary magmatism in southeastern Arizona, *in* Callender, J. F., Wilt, J.C., and Clemons, R.E., eds., Land of Cochise: Socorro, New Mexico Geological Society 29th Field Conference Guidebook, p. 231-241.

Shafiqullah, M., Damon, P.E., Lynch, D.J., Reynolds, S.J., Rehrig, W.A., and Raymond, R.H., 1980, K-Ar geochronology and geologic history of southwestern Arizona and adjacent areas: Arizona Geological Society Digest, v. 12, p. 201-260.

Simons, F.S., 1974, Geologic map and cross sections of the Nogales and Lochiel Quadrangles, Santa Cruz County, Arizona: U.S. Geological Survey Miscellaneous Investigations Series Map I-762, scale 1:24,000, with 9 p. text.

Slaff, Steve, 1993, Land subsidence and earth fissures in Arizona, Arizona Geological Survey Down-to-Earth Series 3, 24 p.

Smith, C.H., 1989, Geologic map of the Little Rincon Mountains: Arizona Geological Survey Contributed Map CM-89-C, 1 sheet, scale 1:10,000.

Spencer, J. E., Ferguson, C. A., Richard, S. M., Orr, T. R., Pearthree, P. A., Gilbert, W. G., and Krantz, R. W., 2002 (Revised), Geologic Map of The Narrows 7.5' Quadrangle and the Southern Part of the Rincon Peak 7.5' Quadrangle, Eastern Pima County, Arizona: Tucson, Arizona Geological Survey Digital Information Series DGM-10, 32 pages, one sheet, in Adobe Acrobat (.pdf) format, 1 CDROM, design scale 1:24000.

Spencer, J.E., and Reynolds, S.J., 1989, Middle Tertiary tectonics of Arizona and the Southwest, *in* Jenney, J.P., and Reynolds, S.J., eds., Geologic evolution of Arizona: Arizona Geological Society Digest, v. 17., p. 539-574.

Spencer, Jon E., and Welty, John W., 1989, Geology of mineral deposits in the Buckskin and Rawhide Mountains, *in* Spencer, Jon E., and Reynolds, Stephen J., eds., Geology and Mineral Resources of the Buckskin and Rawhide Mountains, West-central Arizona: Tucson, Arizona Geological Survey Bulletin 198, p. 223-254.

Streckeisen, A.L., 1973, Plutonic rocks: Classification and nomenclature recommended by the IUGS Subcommission on the Systematics of Igneous Rocks: Geotimes, v. 18, n. 10, p. 26-30.

U.S. Geological Survey, 2001, Real-time data for selected stream gaging sites in Arizona website; annual peak flow data.

Wilkinson, William H., Wendt, Clancy J., and Dennis, Michael D., 1988, Gold mineralization along the Riverside Mountains Detachment Fault, Riverside County, California, *in* Schafer, Robert W., Cooper, James J., and Vikre, Peter G., Editors, Bulk Mineable Precious Metal Deposits of the Western United States, Symposium Proceedings: Reno, NV, The Geological Society of Nevada, p. 487-503.

Western Regional Climate Center, 2001, Arizona climate summaries, in Western U.S. historical climate summaries, WRCC Web Page, Desert Research Institute, University of Nevada.

Wood, M.L., House, P.K., and Pearthree, P.A., 1999, Historical geomorphology and hydrology of the Santa Cruz River: Arizona Geological Survey Open-File Report 99-13, 98 p., 1 sheet, scale 1:100,000.

Wrucke, C.T., 1989, The middle Proterozoic Apache Group, Troy Quartzite, and associated diabase of Arizona, *in* Jenney, J.P., and Reynolds, S.J., eds., Geologic Evolution of Arizona: Arizona Geological Society, Digest 17, p. 239-258.

Yen, T, 1951, Fresh-water mollusks of Cretaceous age from Montana and Wyoming: U. S. Geological Survey Professional Paper 233-A, 20 pp.